NASA TN D-333

IN-02
381829

NASA

TECHNICAL NOTE

D-333

LARGE-SCALE WIND-TUNNEL TESTS AND EVALUATION OF
THE LOW-SPEED PERFORMANCE OF A 35° SWEPTBACK
WING JET TRANSPORT MODEL EQUIPPED WITH
A BLOWING BOUNDARY-LAYER-CONTROL
FLAP AND LEADING-EDGE SLAT

By David H. Hickey and Kiyoshi Aoyagi

Ames Research Center
Moffett Field, Calif.

NATIONAL AERONAUTICS AND SPACE ADMINISTRATION

WASHINGTON   October 1960

NATIONAL AERONAUTICS AND SPACE ADMINISTRATION

TECHNICAL NOTE D-333

LARGE-SCALE WIND-TUNNEL TESTS AND EVALUATION OF
THE LOW-SPEED PERFORMANCE OF A 35° SWEPTBACK
WING JET TRANSPORT MODEL EQUIPPED WITH
A BLOWING BOUNDARY-LAYER-CONTROL
FLAP AND LEADING-EDGE SLAT

By David H. Hickey and Kiyoshi Aoyagi

SUMMARY

A wind-tunnel investigation was conducted to determine the effect of trailing-edge flaps with blowing-type boundary-layer control and leading-edge slats on the low-speed performance of a large-scale jet transport model with four engines and a 35° sweptback wing of aspect ratio 7. Two spanwise extents and several deflections of the trailing-edge flap were tested. Results were obtained with a normal leading-edge and with full-span leading-edge slats.

Three-component longitudinal force and moment data and boundary-layer-control flow requirements are presented. The test results are analyzed in terms of possible improvements in low-speed performance. The effect on performance of the source of boundary-layer-control air flow is considered in the analysis.

INTRODUCTION

A wind-tunnel investigation of the low-speed characteristics of a large-scale jet transport model with four pylon-mounted engine nacelles on a 35° sweptback wing of aspect ratio 7 was reported in reference 1. In that investigation, various leading-edge devices, including leading-edge slats and a leading edge with modified radius and camber, were studied in conjunction with double-slotted trailing-edge flaps. In reference 2, it was shown that blowing-type boundary-layer control applied to trailing-edge flaps in conjuction with a full-span leading-edge slat should provide significant improvements in the take-off and landing performance of an airplane with a 35° sweptback wing of aspect ratio 6.75 and two pylon-mounted engine nacelles.

In view of the possible need for shorter take-off distances and slower landing speeds of future jet transport or cargo airplanes, additional wind-tunnel investigations of the large-scale jet transport model

of reference 1 were conducted with blowing boundary-layer control applied
to plain trailing-edge flaps. Leading-edge slats were used to control
leading-edge separation. The purpose of the investigation was to deter-
mine the flow requirements for boundary-layer control and the practica-
bility of using boundary-layer control over a limited range of take-off
thrust to weight ratios. Estimations are made of take-off and landing
performance with boundary-layer-control air supplied both by engine bleed
and an auxiliary compressor; thus, effects of thrust loss due to engine
bleed were included in the calculations. The performance calculations
are based on the requirements for turbine-powered transports specified in
reference 3.

Three-component force and moment data are presented for various
configurations of trailing-edge flaps and leading-edge slats. The tests
were conducted in the 40- by 80-foot wind tunnel of the Ames Research
Center at a Reynolds number of 4.2×10^6.

NOTATION

A_n nozzle area, sq in.

b   wing span, ft

BLC   boundary-layer control

c   chord, measured parallel to the plane of symmetry, ft

$\bar{c}$ mean aerodynamic chord, $\dfrac{2}{S} \displaystyle\int_0^{b/2} c^2 dy$, ft

C_D drag coefficient, $\dfrac{\text{drag}}{q_\infty S}$

C_L lift coefficient, $\dfrac{\text{lift}}{q_\infty S}$

C_m pitching moment about $0.30\ \bar{c}$, $\dfrac{\text{pitching moment}}{q_\infty S \bar{c}}$

C_μ momentum coefficient, $\dfrac{W_j/g}{q_\infty S} V_j$

D   drag, lb

F_G static thrust, lb

F_n net thrust from engine, $\dfrac{W_e V_{TP}}{g} - \dfrac{W_e V_\infty}{g}$, lb

g	acceleration of gravity, 32.2 ft/sec^2
L	lift, lb
LE	leading edge
l_t	distance from the quarter-chord point of the wing mean aerodynamic chord to the quarter chord of the horizontal-tail mean aerodynamic chord
p	static pressure, lb/sq ft
p_t	total pressure, lb/sq ft
q	dynamic pressure, lb/sq ft
S	wing area, sq ft, or total take-off distance, ft
S_f	wing area spanned by flaps, sq ft
S_G	take-off ground roll, ft
T	temperature, $^{\circ}$R
TE	trailing edge
V	velocity, ft/sec or knots
V_{LO}	velocity at lift off, knots
V_S	stalling speed, ft/sec or knots
V_j	jet velocity, assuming isentropic expansion, ft/sec
V_{TP}	velocity at exit of engine tail pipe, ft/sec
W	gross weight, lb, or weight rate of flow, lb/sec
x	streamwise distance along airfoil chord, ft
y	spanwise distance perpendicular to the plane of symmetry, ft
z	perpendicular distance above the extended wing-chord plane, ft
α	angle of attack of fuselage reference line, deg
Λ_{HL}	sweepback angle of flap hinge line, deg
Δ	incremental value

δ_f flap deflection measured normal to the flap hinge line, deg

δ_s slat deflection measured from wing chord line

η wing semispan station, $\frac{2y}{b}$

μ rolling friction coefficient

Subscripts

b   bleed air flow

d   flap duct

2D   two-dimensional

3D   three-dimensional

e   engine air flow

g   in ground effect

j   flap jet

l lower

∞ free stream

R   rotation

to   take off

u   upper

MODEL AND APPARATUS

Figure 1 is a photograph of the model as installed in the 40- by 80-foot wind tunnel. Pertinent dimensions of the model are given in figures 2 and 3.

Wing

The wing was sweptback 35° at the quarter-chord line. It had an aspect ratio of 7, a taper ratio of 0.3, a dihedral of 6°, and an incidence of 2°. An NACA 65A414 airfoil section was employed at the root, with a straight taper to the 65A410 section at the tip (see table I for ordinates).

A leading-edge slat was contained in the wing. A typical slat-wing cross section is shown in figure 3 and the slat ordinates are listed in table II. Slat breaks at each engine pylon were provided, so that each segment of the slat could be individually extended. When the slat was extended, it was deflected 15° from the wing-chord plane. Unless otherwise specified, all three slat segments were deflected together.

Trailing-Edge Flap System

The wing-flap geometry and a typical cross section of the flap are shown in figure 3.

Flap details.- The trailing-edge flap was designed to be contained in the aft 40 percent of the wing. The plain flap was hinged at 68-percent chord, and the boundary-layer-control (BLC) ducting was placed within the flap. The blowing nozzle was on the flap radius 35° from the perpendicular to the flap chord line. A nozzle height of 0.020 inch was used throughout the investigation. Provisions were made for flap deflections from 0° to 60°.

The flap was constructed in three spanwise segments. The divisions occurred at 9-, 34-, 44-, and 63-percent semispan at the wing trailing edge. Flap deflections with the flap segment from 34- to 44-percent semispan undeflected will be referred to as the interrupted-span flap; when all three segments of the flap are deflected, the flap will be described as the continuous-span flap.

Boundary-layer-control air supply.- Air for BLC was provided by a centrifugal pump driven by electric motors. This unit was installed in the model fuselage. The air exiting from the blower was conducted to a plenum chamber, and from there to the flap on either side of the model by means of separate ducts. Each duct to the flap had a calibrated flow measuring station consisting of total head tubes, static orifices, and a thermocouple.

Fuselage

The fuselage cross section was defined by a 4- by 5-foot ellipse, except for the nose section and tail cone. The nose section was one-half of a 4- by 8-foot ellipse in the horizontal cross section and of a 5- by 8-foot ellipse in the vertical cross section. The tail cone had a straight taper from a 4- by 5-foot ellipse to a similar but smaller ellipse at the tail.

Nacelles and Pylons

Engine nacelles and pylons were attached to the wing at 40- and 70-percent semispan. The nacelles were designed to house J-30 engines. The pylons were 4-1/8 inches thick with faired leading and trailing edges. The pylons and engine nacelles were on the model throughout the investigation. Since the engines were not operated during the present investigation, plugs were installed in the engine inlets.

Tail

Geometry of the horizontal and vertical tails is given in figure 2. Both horizontal and vertical tails were fixed at 0° during the investigation and were on the model throughout the investigation.

TESTING AND PROCEDURE

Force and moment data were obtained through an angle-of-attack range from -4° to +19°. All tests were conducted at a free-stream airspeed of 93 feet per second, corresponding to a Reynolds number of 4.2×10^6 and a dynamic pressure of 10 pounds per square foot.

Tests With Constant C_μ and Varying Angle of Attack

When angle of attack was varied while the boundary-layer control was operating, C_μ was maintained at a level adequate to keep attached air flow on the flap. Two trailing-edge flap spans and several deflections in combination with leading-edge slats were tested. Only the highly deflected interrupted flap was tested with the leading-edge slats retracted.

Tests With Constant Angle of Attack and Varying C_μ

Momentum coefficient was varied, with α held constant, on both interrupted and continuous span trailing-edge flaps for deflections from 30° to 60°. In general, the data were obtained with the leading-edge slats extended. Comparable data were also obtained with 30° and 40° of flap deflection, with the model near a simulated ground plane.

CORRECTIONS

The following corrections for the effect of wind-tunnel boundaries were applied, except when the model was tested in ground effect.

$$\Delta\alpha = 0.59 \ C_L$$

$$\Delta C_D = 0.010 \ C_L^2$$

$$\Delta C_m = 0.0028 \ C_L$$

RESULTS AND DISCUSSION

This investigation was directed at improving the low-speed performance and increasing the lift capabilities of a typical four-engined jet-transport-type airplane by application of blowing-type boundary-layer control (BLC) to trailing-edge flaps in conjunction with leading-edge slats. The first section of the experimental portion of the report will show typical aerodynamic characteristics of the model with BLC applied to two spanwise extents of trailing-edge flaps and with leading-edge slats extended. The second section will show the BLC momentum coefficient requirements for various deflections of the trailing-edge flaps.

Typical Aerodynamic Characteristics

Trailing-edge flaps undeflected.- The lift, drag, and pitching-moment characteristics of the jet transport model with trailing-edge flaps undeflected and leading-edge slats retracted are shown in figure 4, and are compared to results obtained from the same model during the investigation reported in reference 1. A significant difference exists in the data, particularly in the high angle-of-attack range; in the present investigation the maximum lift coefficient is 0.15 less than that reported in reference 1. The increase in drag with increased lift coefficient near maximum lift coefficient is also much larger for the model in the present tests. The reason for the difference was determined to be a distortion of

the wing leading-edge contours in the region of the nacelle pylons which
was not corrected. The discrepancy in test results caused by this dis-
tortion interferes with any direct comparison of test results near maximum
lift from the investigation of reference 1 and the present investigation.

Trailing-edge flaps deflected.- The lift, drag, and pitching moment
for both the interrupted and continuous spanwise extents of trailing-edge
flap at several flap deflections and with leading-edge slats extended
are shown in figure 5. The results reported in reference 2 for an airplane
with a similar wing plan form indicated that with blowing BLC and with
full-span leading-edge slats, considerably higher increments of maximum
lift could be obtained than were measured in the present study. Observa-
tions of wing tufts in the present investigation indicated that stall
occurred at 4° to 5° lower angle of attack on the right wing panel than
on the left wing panel, resulting in maximum lift coefficients of approxi-
mately 0.35 lower than expected with large flap deflections. It is likely
this is a consequence of the wing distortion noted earlier. Thus, con-
clusions based on the present data with respect to the effect of BLC and
leading-edge slats on performance are expected to be conservative.

It has been shown previously, for example in reference 2, that the
full value of high-lift devices is realized only when control of leading-
and trailing-edge air-flow separation is properly balanced; the maximum
allowable ground angle plays an important part in the determination of
this balance. The data (fig. 5) with 40° BLC flaps show that if the air-
craft were to take off at the maximum ground clearance angle (usually 6°
to 8° angle of attack), the stall-speed margin would be considerably less
than the 20-percent requirement. Thus, in order to use the 40° BLC flap
effectively, better control of leading-edge stall would be required.
These comments are intended to emphasize the care that must be taken to
balance the stall control on the wing leading edge and trailing edge in
order to avoid useless complication or excessive performance penalties.

The effect of various leading- and trailing-edge configurations is
shown by the data in figure 6.

The variation of BLC flap lift increment with flap deflection for
the two spanwise extents of trailing-edge flaps is shown in figure 7,
along with estimated lift calculated by the method of reference 4.
Also included are the measured values of large extended chord double-
slotted flaps on the same model, and the increments obtained in flight
with smaller chord double-slotted flaps. The data presented for the
large chord double-slotted flaps were obtained during the investigation
reported in reference 1; however, the tail-off lift increments for the
interrupted-span flap were not previously published. Data for the
smaller chord flap came from the flight investigation of the KC-135
(ref. 5). The flap lift increments shown in figure 7 for the BLC and
small-chord double-slotted flaps were obtained by correcting the measured
tail-on lift increments for the tail download due to downwash. The theory
of reference 4 shows fairly good agreement with the measured values, in
most cases underestimating the lift increment by less than 10 percent.

With the BLC flaps of 0.32 chord ratio the measured values of flap lift increment are 20 to 60 percent larger, depending on flap span and deflections, than those obtained with the large-chord, extended, double-slotted flap of 0.495 total flap chord ratio.

The incremental lift-drag ratios due to flap deflection at 0° angle of attack are shown in figure 8 for the BLC flap and double-slotted flaps for a range of flap deflections and the two spanwise extents of trailing-edge flaps. As in the case of the flap lift increments, the values of lift-drag-ratio increments are for the horizontal tail off to give a more direct comparison. For both extents of flap span shown, the lift-drag-ratio increment due to flaps at 30° deflection is approximately 100 percent higher with the BLC flap than with the large-chord double-slotted flap. At 60° deflection, the lift-drag-ratio increments due to both the BLC and double-slotted flap are essentially equal. For the continuous-span flap (0.09 to 0.63 semispan) the lift-drag-ratio increments are slightly higher than for the interrupted span flap for both the double-slotted and BLC flap at all flap deflections.

Comparison of pitching moments with the BLC flap, shown in figure 5, with the results for the double-slotted flap of reference 1 for equivalent flap deflections and horizontal-tail incidence indicates that BLC flaps for a given lift coefficient have considerably less moment to trim for balance. This difference is due to the increased downwash on the tail with the BLC flap (discussed in ref. 6), the extended chord of the double-slotted flaps with the associated increase of wing area aft of the center of gravity, and the difference in angle of attack at the same lift coefficient. An unstable variation of pitching moment is indicated at or near maximum lift coefficient with the BLC flap and full-span leading-edge slats (fig. 5). A similar characteristic can be noted with the double-slotted flap as indicated by the results reported in reference 1. However, as shown in figure 6, partial span extents of leading-edge slats should give a stable variation of pitching moment at maximum lift but at the cost of lower maximum lift coefficients than with full-span slats.

Boundary-Layer-Control Requirements

The momentum coefficient, C_μ, required for BLC on the plain flap of the jet transport is generally similar to the requirement predicted from the results of the investigations reported in references 2 and 7. Typical variations of the lift coefficient with momentum coefficient for the two spanwise extents of flap and several flap deflections are shown in figure 9. The critical values of C_μ for BLC, as determined by flap surface pressure distributions, are indicated by tick marks on the curves. These values vary from 0.008 to 0.018, depending on flap deflection, for the interrupted-span flap, and 0.012 to 0.024 for the continuous-span flap.

10

In order to compare momentum coefficients of the jet transport model with those in references 2 and 7, the equivalent two-dimensional values are presented in figure 10. These values were computed by the expression from reference 7

$$C_{\mu 2D} = \frac{C_{\mu 3D}(S/S_f)}{\cos^2\Lambda_{HL}}$$

The equivalent two-dimensional values for both spanwise extents of BLC flap for the jet transport model were 50 to 60 percent larger than for the airplanes of references 2 and 7. This is at least partially due to the larger ratio of flap chord to wing chord (0.32 compared to 0.23) of the blowing flap of this investigation.

A
3
4
0

PERFORMANCE EVALUATION

Take-off performance was calculated for a hypothetical jet transport with a wing loading of 100 pounds per square foot; two thrust to weight ratios, 0.206 and 0.250, were used to represent a probable range of take-off thrust to weight ratios of future subsonic jet transports. The trim lift-drag polars that were used for the take-off calculations are shown in figure 11 for the blowing and double-slotted interrupted flap with various deflections. Also shown are unpublished data for the double-slotted flap obtained during the investigation reported in reference 1. Although the KC-135 performance characteristics will be compared with the blowing flap model characteristics, it should be noted that the KC-135 and model results with a double-slotted flap are nearly the same at a flap deflection of 30°. Hereinafter, when double-slotted flaps are considered, it will be understood that the results are based on the KC-135 characteristics. Further details of the take-off calculations are in appendix A.

Two methods are considered for reducing thrust loss due to air bled from the engines for boundary-layer control. The first method (discussed in ref. 2) is to have a two-position valve in the BLC ducting, one position for landing and another for take-off, to allow a restricted amount of air to be bled from the engine during the take-off ground roll. This method would result in an essentially constant thrust loss during the ground roll and an unnecessarily large excess of air bled from the engine (and thrust loss) during a major portion of the ground roll where the velocity is less than the BLC design velocity. The second method reduces this thrust loss by programming the air bled from the engine with velocity. In this calculation the amount of bleed air was programmed in three velocity steps, the result being a 50- to 60-percent average reduction of thrust loss. Details of these calculations are given in appendix B. Use of an auxiliary compressor is a third method of supplying BLC air. The assumed compressor weight penalty of 1000 pounds for the calculation could be reduced by

utilizing the compressor for several purposes, such as de-icing, auxiliary high pressure air supply for an engine starter, or as a source of air supply for other auxiliary equipment.

Take-Off Performance

A
3
4
0

Take-off ground roll.- The method used to calculate the take-off ground roll is the same as discussed in reference 2 and appendix A. To evaluate the accuracy of the method, calculations were made for the KC-135 airplane based on flight measurements of lift and drag (ref. 5) for 30° of flap deflection. In figure 12 the results of the calculated values are compared to the measured values from reference 8 and indicate that the method gave reliable estimates of take-off ground-roll distance for the range of thrust to weight ratios available for comparison (from 0.185 to 0.230).

The results of the calculations of the ground-roll distance required to accelerate to take-off velocity are shown in figures 13, 14, and 15 for various flap deflections, angles of rotation at take-off, and thrust to weight ratios. The results, shown in figures 13 and 14 for a range of angles of attack at take-off varying from 0° to 8°, indicate that significant reductions in take-off ground roll can be obtained with BLC and leading-edge slats; the largest gains occur at the lower rotation angles for take-off. Although this conclusion is based on comparison with KC-135 results, a similar conclusion could be based on the 30° large-chord double-slotted flap results because, as stated previously, the double-slotted flap model and KC-135 characteristics are similar with 30° of flap deflection. The results also indicate that the rotation angles at take-off can be reduced by about 3° to 5° for a comparable take-off distance with BLC, particularly with programmed bleed or an auxiliary compressor. The importance of rotation angle during take-off is discussed in reference 9. Since the ground-roll distance required to accelerate to take-off velocity was shorter with high-lift devices and the take-off velocity was less, the accelerate-stop distance also should be significantly less. Figure 15 summarizes the results of figures 13 and 14 for an angle of rotation of 6°, which is near the value that was indicated in reference 8 to be the rotation angle for best take-off performance of the KC-135.

In the following table the results are compared for 40° deflection with BLC applied by the three methods and for 30° double-slotted flap deflection; take-off ground roll is listed for two angles of rotation and two thrust to weight ratios.

Configuration	Angle of·attack at take-off, deg	Ground-roll distance, S_G, ft	
		$F_G/W=0.206$	$F_G/W=0.25$
Double-slotted flaps; $\delta_f = 30^\circ$	2 6	11,250 7,000	8,300 5,400
BLC flaps; $\delta_f = 40^\circ$; large thrust loss; two-position valve control of air bleed from engines	2 6	8,200 5,850	5,850 4,300
BLC flaps; $\delta_f = 40^\circ$; small thrust loss; programmed air bleed from engines	2 6	7,350 5,300	5,350 4,000
BLC flaps; $\delta_f = 40^\circ$; no thrust loss; auxiliary compressor	2 6	7,050 5,050	5,150 3,850

A large reduction in ground-roll distance to take-off velocity would be obtained with 40° of flap deflection with the engine bleed controlled by a two-position bleed valve. Programmed bleed or an auxiliary compressor BLC air supply would provide a further reduction of take-off ground-roll distance compared to that obtained with the two-position bleed ducting valve. These methods of applying BLC may also be desirable from a climb-out standpoint after take-off or may be a necessary improvement for airplanes with low thrust to weight ratio.

Take-off climbout performance.- Although it appears that significant reductions in take-off ground-roll distance can be made with BLC trailing-edge flaps used in conjunction with leading-edge slats, consideration must also be given to the climbout after take-off for both the four-engine case and the one-engine-inoperative case. The method used and the assumptions made in calculating the climbout performance are discussed in appendix A and are based on requirements set forth in reference 3. Longitudinal characteristics assumed in the calculations are presented in figure 11. In making the calculations it was assumed that the airplane was accelerated on the ground to take-off velocity, then rotated to the angle of attack for $1.2 V_S$ (6° with 30° of flap deflection and 4° with 40° of flap deflection) at which time lift-off would occur. Both the velocity of rotation and the lift-off velocity are dependent on the requirement that $1.2 V_S$ must be reached prior to 35 feet of altitude. It was also assumed that the drag due to extended landing gear would exist for 10 seconds after lift-off. To study the trends of climbout performance with one engine inoperative, it was assumed that the engine lost power at lift-off speed.

The results of the calculations are shown in figures 16, 17, 18, and 19 for thrust to weight ratios of 0.206 and 0.250 for the four-engine and the one-engine-inoperative cases. For each of the conditions results are shown for applying BLC with an auxiliary compressor and by bleeding air from the jet engines (programmed during ground roll). For the thrust to weight ratio of 0.250 (figs. 16 and 17) considerable improvement over the aircraft with the double-slotted flap is shown with BLC and leading-edge slats for either an auxiliary compressor or air bleed from the engine. Total take-off distance including climbout to 35 feet altitude was reduced 1350 to 1700 feet depending on the trailing-edge-flap deflection and the method of applying BLC. With an auxiliary compressor for boundary-layer control, the distance to 35 feet was reduced 1650 feet and the climb gradient at 1.2 V_S was greater than for the aircraft with the double-slotted flap. Thus, even with the distorted slats, a large gain in take-off performance is indicated. The lowest climb gradient was with bleed air from the engines for BLC and one engine inoperative, the gradient being about 5.0 percent, which would exceed the minimum required by reference 3.

For a thrust to weight ratio of 0.206 (figs. 18 and 19) reductions of 1200 to 2400 feet in take-off distance to 35 feet altitude compared with the double-slotted flap aircraft appear possible with leading-edge slats and with boundary-layer control flap deflected 30°. With one engine inoperative, 40° of flap deflection, and air bleed from the engines for BLC, the climbout performance would be unacceptable because of a climb gradient of only 1.3 percent; with an auxiliary compressor for BLC, the climbout gradient of 3 percent would be marginal.

It should be noted that the calculations with the 40° flap were confined to a rotation angle of 4° because of the inadequate leading-edge stall control afforded by the distorted slats. With more efficient leading-edge protection, so that 6° of rotation could be used (as was the case for the 30° BLC flap), all distances with 40° of flap deflection on figures 16 through 19 would be reduced 600 to 900 feet. However, as the climb gradient is virtually unaffected by this change in attitude, the climb gradient limitations would be the same.

The climb gradients for the various configurations for the four-engine case and the one-engine-inoperative case are given in the following table for landing gear up out of ground effect.

Trailing-edge flap configuration	Climb gradient, percent			
	Four engine		One engine inoperative	
	Basic $F_G/W=0.206$	Basic $F_G/W=0.250$	Basic $F_G/W=0.206$	Basic $F_G/W=0.250$
$\delta_f = 30^o$, double slotted	10.0	15.0	4.9	8.0
$\delta_f = 30^o$ BLC, air bleed from engines	9.6	13.8	4.2	7.5
$\delta_f = 30^o$ BLC, auxiliary compressor	10.9	15.8	5.8	9.1
$\delta_f = 40^o$ BLC, air bleed from engines	6.3	10.6	1.3	5.0
$\delta_f = 40^o$ BLC, auxiliary compressor	8.0	12.5	3.0	6.2

In terms of climb gradient it appears that at thrust-to-weight ratios less than 0.206, the performance of the aircraft with one engine inoperative, with BLC flaps, and air bled from the engines would be marginal or unsatisfactory. It probably would be necessary to use either an auxiliary compressor for boundary-layer control or flap deflections of the order of 30° to meet the required 3-percent climb gradient.

Effect of BLC on payload.- Another aspect of performance is the runway-limited payload of an aircraft. The comparison was made for a take-off ground-roll distance of 6000 feet and a total thrust available for take-off of 50,000 pounds. It was assumed that the basic weight with fuel but with no payload was 200,000 pounds and the weight of the auxiliary compressor for boundary-layer control was 1000 pounds. The results are shown in the following table for three BLC conditions.

Configuration	6000-foot take-off ground roll		
	Payload, lb	F_G/W	One-engine inoperative-climb gradient
Double-slotted flaps, $\delta_f = 30°$	29,500	0.220	Satisfactory (6 percent)
BLC flaps, $\delta_f = 30°$, auxiliary compressor	47,000	.202	Satisfactory (5.6 percent)
BLC flaps, $\delta_f = 40°$, auxiliary compressor	62,000	.181	Unsatisfactory (1.8 percent)
BLC flaps, $\delta_f = 30°$, programmed air bleed from engines	43,000	.206	Marginal (3 percent)

It should be noted that the increased payload may not all be useful since additional fuel would be required to carry the additional load to a given altitude and distance. The increased payload listed for the 30° BLC flap and auxiliary blowing system reduces absolute range about 5 percent. If range is kept constant, about 25 percent of the allowable weight increase must be used for fuel. If all the weight increase were used for fuel, absolute range would be increased 20 percent.

Landing Approach Speed

In view of the jet transport regulations that the landing approach speed be not less that 1.3 V_S, the effect of the BLC flap and leading-edge slats on landing will be evaluated on the basis of this minimum approach speed. The curves shown in figure 20 indicate, for several landing configurations, the variation of thrust to weight ratio with velocity required for 1 g zero sink flight at a wing loading of 65 pounds per square foot. Data for both boundary-layer-control flaps at various deflections and double-slotted flaps at 50°, which is the approximate flap deflection used in the final stages of the landing approach of the KC-135, are included in the figure. The values of 1.3 V_S are indicated on the curves of figure 20 for each flap configuration and are given in the following table with the increment of thrust-to-weight ratio available for climbout, based on the value of 0.206 for take-off (W/S = 100 lb/sq ft), and the appropriate angle of attack for the approach. The effect of thrust loss due to engine bleed for the blowing boundary-layer control is taken into account in the

quoted values of thrust margin with one engine inoperative. With an auxiliary compressor for boundary-layer control, the thrust margin for climbout with one engine inoperative would be larger.

Configuration	Approach speed, k	$\Delta F_n/W$, thrust margin one engine inoperative	α, deg
$\delta_f = 50^\circ$, double-slotted flap	147	0.07	3.5
$\delta_f = 30^\circ$, BLC flaps and leading-edge slats	135	.116	3.0
$\delta_f = 40^\circ$, BLC flaps and leading-edge slats	128	.09	.5
$\delta_f = 50^\circ$, BLC flaps and leading-edge slats	122	.06	-.5

The results indicate that with the landing gear down, the thrust margin for "go around" at all flap deflections with BLC is nearly equal to or larger than the thrust margin with double-slotted flaps. Flight tests of aircraft with blowing BLC indicated additional gains in handling qualities not measurable in wind-tunnel tests. These results are discussed in reference 10. The effect of BLC on control characteristics is discussed in reference 6.

The results in the above table indicate that a 12 to 25 knot reduction should be obtainable in landing approach speeds with the use of a boundary-layer-control flap and leading-edge slats compared with the double-slotted flap configuration depending on the flap deflection and thrust margin desired. For the 30° BLC flap and 50° double-slotted flap deflections the fuselage attitudes would be about 3° above the glide-slope angle relative to the ground so that approach speed probably could not be reduced below the values shown even if maximum lifts were higher. For the 50° BLC flap, substantial further reductions in approach speed would be possible if maximum lift were increased sufficiently to allow about a 4° increase in fuselage attitude. Large-scale wind-tunnel tests and flight tests that have been conducted on swept-wing fighter-type aircraft with blowing BLC applied to a leading-edge flap (see ref. 11) indicate that considerable improvement in maximum lift and reduction in the increase of drag at high lift coefficients can be obtained compared to normal wing leading edges or leading-edge slats. Shown on figure 20 is an estimated curve, based on the results of this reference that indicate the effects of leading-edge flap blowing BLC. The estimated curve is for

the landing configuration with 50° of blowing flap deflection. The estimation shows that leading-edge BLC reduces stalling speed and maintains a stable variation of F_n/W versus airspeed to below the approach speed. Provided that these effects can be produced on the jet transport as they have been on swept-wing fighter aircraft, the 1.3 V_S approach speed can be reduced to about 110 knots with an approach angle of attack of about 3° and an 0.075 thrust margin for climbout; this thrust margin is comparable to that shown in the table for double-slotted flaps, but at 37 knots lower speed.

CONCLUDING REMARKS

Large-scale wind-tunnel tests of a typical 35° swept-wing jet transport model indicate that blowing-type boundary-layer control applied to trailing-edge flaps and used in conjunction with leading-edge slats should improve take-off and landing performance.

An evaluation of the results in terms of calculated take-off performance, using flight tests of a similar airplane with double-slotted flaps as a basis of comparison, indicates a possible 20-percent reduction in take-off distance to 35 feet of altitude with satisfactory climb gradients for turbine-powered aircraft; with regard to landing, it appears that landing approach speeds can be reduced by 20 to 25 knots. The analysis shows that for thrust to weight ratios greater than 0.21, supply of the boundary-layer-control air by either engine bleed or an auxiliary compressor should give significant reductions in take-off distance with satisfactory climb gradients when one engine is inoperative. For the take-off flap deflections considered here and thrust to weight ratios less than 0.21, an auxiliary compressor may be required to assure satisfactory climb gradients when one engine is inoperative.

Ames Research Center
    National Aeronautics and Space Administration
        Moffett Field, Calif., June 10, 1960

APPENDIX A

METHOD USED FOR TAKE-OFF AND CLIMBOUT CALCULATIONS

For calculations of the take-off performance the airplane was assumed to have the same geometry as the wind-tunnel model of the subject investigation with the wing area scaled up to 2430 square feet. The take-off wing loading was assumed to be 100 pounds per square foot with 1,000 pounds of additional weight when an auxiliary compressor was used for boundary-layer control. The engine thrusts were chosen for take-off thrust to weight ratios of 0.206 and 0.250. No attempt was made to consider the effect of the variation of thrust to weight ratio during ground roll from zero velocity to take-off speeds. Since this variation should be similar for all cases, the trends shown should be indicative of incremental gains or losses in take-off performance. The drag value flaps up and the drag of the landing gear were determined from flight test values of the KC-135 (refs. 5 and 8). The flap span used was the interrupted flap span of 0.09- to 0.34-percent semispan and 0.44- to 0.63-percent semispan which is similar to the spanwise extent of flaps of the KC-135.

The equation from reference 2, used to calculate ground-roll distance required to accelerate to take-off velocity, is as follows:

$$S_G = \frac{13.1 \ W/S}{C_{L_g}\left(\frac{D}{L} - \mu\right)} \ ln \ \frac{F_n/W - \mu}{\dfrac{F_n}{W - \mu} - \dfrac{C_{L_g}}{C_{L_{to}}}\left(\dfrac{D}{L} - \mu\right)}$$

The values of C_{L_g} and $C_{L_{to}}$ as well as the D/L were obtained from the trim lift drag polars with flaps and gear down, shown in figure 11, and adjusted for ground effect. The ratios of the values in ground effect to those out of ground effect, computed by the method in reference 12, were estimated to be 1.15 for lift and 1.32 for L/D. Subsequent tests of the model in ground effect indicate these values are probably conservative for the model with the blowing flap. The ground-effect tests were made with the model at essentially take-off ground-roll height and attitude over a ground plane in the 40- by 80-foot wind tunnel. The results in figure 21 show the variation of C_L and L/D with blowing momentum coefficient for the interrupted-span flap at 30° and 40° deflection. The wind-tunnel results indicate an increase in C_L of about 15 to 20 percent and an increase in L/D of 75 to 90 percent, depending on flap deflection and C_μ, with the airplane in ground effect. These values for L/D are considerably greater than used in the calculations. In order to keep the calculated results conservative, the lower values were used in the performance calculations. Ground effect was assumed to extend only to 35 feet of altitude. The ground resistance friction coefficient was assumed

to be 0.01, which was determined from reference 13 where measurements were made with various tire pressures. When boundary-layer control was obtained by bleeding air from the jet engines, the thrust to weight ratio available for take-off was corrected to include the thrust loss.

The take-off ground roll was made at 0° fuselage angle with rotation to various angles between 0° and 8° at the appropriate take-off velocity. A rotation rate of 2° per second was used for the cases where climbout was considered. This assumption of rotation rate was necessary in view of the changes to the Civil Air Regulations presented in reference 3 defining the rotational velocity, V_R, and the lift-off velocity, V_{LO} as dependent on the requirement the $1.2\ V_S$ be attained prior to reaching 35 feet of altitude. It was also assumed that the drag due to landing gear would exist for 10 seconds after lift-off. For the three-engine case it was assumed that the thrust of one engine was lost just at the lift-off point in order to indicate the three-engine climbout performance and climb gradient.

The climbout after take-off was calculated in three phases. First, the airplane was accelerated to $1.2\ V_S$ prior to reaching 35 feet of altitude; second, continuous climb at $1.2\ V_S$ (6° angle of attack) with wheels down extended for a time of 10 seconds after the lift-off point; and third, climbout with wheels up at $1.2\ V_S$ was continued to 400 feet with no other changes made on take-off configuration. Although differences may exist in actual practice of take-off and climbout of jet transports, the method used in making the calculations should indicate the incremental gains or losses in performance.

APPENDIX B

METHOD OF BOUNDARY-LAYER-CONTROL SYSTEM DESIGN

References 2 and 7, which report the results of blowing-type boundary-layer control applied to trailing-edge flaps, discuss the procedure used to determine the air-flow and pressure-ratio requirement for boundary-layer-control flaps. The discussion in reference 7 relates the matching of engine compressor air bleed characteristics with the airplane velocity, boundary-layer-control air-pressure ratio and weight rate of flow requirements, and nozzle areas for a given required momentum coefficient. The discussion in reference 2 relates the same variables but treats the problem of using BLC for take-off and landing. A two-position pressure valve was suggested to control the BLC nozzle pressure ratio at take-off during rated power operation to pressure ratios that are compatible with a BLC nozzle area sized to give satisfactory BLC results at the lower pressure ratios available during the landing approach. Use of this valve results in a reduction of thrust loss due to BLC air bleed during the take-off ground roll. The following discussion includes these variables and the additional variable of a different C_μ required for various flap deflections.

NOZZLE AREA SELECTION

For the hypothetical jet transport considered here, C_μ required for BLC varied from 0.008 for 30° flap deflection to 0.018 for 60° flap deflection. The weight rate of flow and nozzle area required for a range of pressure ratios at a take-off wing loading of 100 pounds per square foot and 30° or 40° flap deflection are shown in figure 22(a). Corresponding values for landing conditions with a wing loading of 65 pounds per square foot and 40° or 50° flap deflection are presented in figure 22(b). A duct pressure ratio of about 4 was chosen as representative of that available from engine compressors during landing approach. This value allows for about 50-percent duct losses. Under these low thrust conditions a nozzle area of 20 square inches (see fig. 22(b)) with a weight rate of flow of 20.5 pounds per second is required to provide BLC for 40° flap deflection. For take-off with this nozzle area, a pressure ratio of 4.5 with a BLC air flow of 21.8 pounds per second is required. With the engines at take-off thrust, a pressure ratio of about 8 would be available; thus a control would be needed to reduce take-off duct pressure ratio in order to avoid the unnecessary thrust loss associated with the excess BLC air bleed. Design of the combination auxiliary compressor and BLC nozzle is concerned primarily with the characteristics of the compressor. As the previously discussed landing and take-off pressure ratios were nearly equal, little compromise would be required to match the two requirements.

REDUCTION OF THRUST LOSSES

Several possible methods can be used to reduce the thrust loss due to bleeding air from the engines. An auxiliary compressor can be carried with its own source of power which will give no thrust loss to the engines but will add to the take-off weight of the airplane and the weight during the entire flight. In the calculation a weight of 1000 pounds was assumed for the compressor. Reference 2 proposed the use of a two-position valve to reduce the thrust loss during take-off; however, as shown in figure 23(a), the C_μ over the flaps from zero forward velocity to take-off velocity would be much greater than actually needed for boundary-layer control, and thus result in an unnecessary thrust loss during the entire ground roll. This thrust loss would be 8 percent (calculated by $\Delta F_n/F_n = 2.5\ W_b/W_e$) with $30°$ flap deflection or 9.8 percent for $40°$ flap deflection, as shown in figure 23(b). Continuously programming the bleed air with velocity would give the ideal C_μ and thrust loss during ground roll as shown in figure 23(b), and would result in an average thrust loss of about 2.8 percent. Programming in steps would be a compromise method and an example is shown in figure 23(b) for three steps. In this case, a constant bleed flow rate would be held from 0 to 50 knots, which would result in excess C_μ over most of this speed range. Thrust loss is, however, considerably less than for the case with a two-position pressure valve. At 50 knots the bleed flow rate would be increased and held constant to 100 knots and finally at 100 knots the full bleed flow rate would be used from 100 knots to take-off and climbout speeds. This would result in an average thrust loss of about 4.6 percent for the entire ground roll compared to an average of 9.0 percent for full bleed during entire ground roll.

REFERENCES

1. Hickey, David H., and Aoyagi, Kiyoshi: Large-Scale Wind-Tunnel Tests
    of a Jet-Transport-Type Model With Leading- and Trailing-Edge High-
    Lift Devices. NACA RM A58H12, 1958.

2. James, Harry A., and Maki, Ralph L.: Wind-Tunnel Tests of the Static
    Longitudinal Characteristics at Low Speed of a Swept-Wing Airplane
    With Blowing Flaps and Leading-Edge Slats. NACA RM A57D11, 1957.

3. Anon.: Special Civil Air Regulation; Turbine-Powered Transport
    Category Airplanes of Current Design. SR-422B, 1959.

4. DeYoung, John, and Harper, Charles W.: Theoretical Symmetric Span
    Loading at Subsonic Speeds for Wings Having Arbitrary Plan Form.
    NACA Rep. 921, 1950.

5. Tambor, Ronald: Flight Investigation of the Lift and Drag Character-
    istics of a Swept-Wing, Multi-Jet, Transport-Type Airplane.
    NASA TN D-30, 1959.

6. Tolhurst, William H., Jr., and Kelly, Mark W.: Full-Scale Wind-
    Tunnel Tests of a 35° Sweptback Wing Airplane With High-Velocity
    Blowing Over the Trailing-Edge Flaps - Longitudinal and Lateral
    Stability and Control. NACA RM A56E24, 1956.

7. Kelly, Mark W., and Tolhurst, William H., Jr.: Full-Scale Wind-
    Tunnel Tests of a 35° Sweptback Wing Airplane With High-Velocity
    Blowing Over the Trailing-Edge Flaps. NACA RM A55I09, 1955.

8. Crawford, Charles C., and Gandy, Charles L., Jr.: KC-135A Heavy
    Weight Take-Off Performance Tests. AFFTC-TR-58-26, Addendum no. 1,
    Oct. 1958.

9. Fischel, Jack, Butchart, Stanley P., Robinson, Glenn H., and Tremant,
    Robert A.: Flight Studies of Problems Pertinent to Low-Speed
    Operation of Jet Transports. NASA MEMO 3-1-59H, 1959.

10. Kelly, Mark W., Anderson, Seth B., and Innis, Robert C.: Blowing-
    Type Boundary-Layer Control as Applied to the Trailing-Edge Flaps
    of a 35° Swept-Wing Airplane. NACA Rep. 1369, 1958.

11. Maki, Ralph L., and Giulianetti, Demo J.: Low-Speed Wind-Tunnel
    Investigation of Blowing Boundary-Layer Control on Leading- and
    Trailing-Edge Flaps of a Full-Scale, Low-Aspect-Ratio, 42° Swept-
    Wing Airplane Configuration. NASA TN D-16, 1959.

A
3
)

12. Goranson, Fabian R.: A Method for Predicting the Elevator Deflection Required to Land. NACA WR L-95, 1944.

13. Pike, E. C.: Coefficients of Friction. The Journal of the Royal Aeronautical Society, vol. 53, no. 468, Dec. 1949, pp. 1085-94.

A
3
4
0

TABLE I.- COORDINATES OF BASIC WING PARALLEL TO THE MODEL PLANE OF SYMMETRY

x_u/c	z_u/c		x_l/c	z_l/c	
	$\eta = 0$	$\eta = 1.0$		$\eta = 0$	$\eta = 1.0$
0	0	0	0	0	0
.00347	.01178	.00842	.00653	-.00945	-.00675
.0058	.01442	.0103	.00920	-.01115	-.00797
.01059	.01853	.01323	.01441	-.01353	-.00967
.02283	.02606	.01862	.02717	-.01738	-.01242
.04757	.03765	.02689	.05243	-.02290	-.01636
.07247	.04678	.03342	.07753	-.02700	-.01928
.09746	.05451	.03893	.10254	-.03038	-.02170
.14757	.06698	.04784	.15243	-.03557	-.02541
.19781	.07656	.05468	.20219	-.03941	-.02815
.24811	.08392	.05994	.25189	-.04215	-.03011
.29846	.08934	.06382	.30154	-.04398	-.03142
.34884	.09299	.06642	.35116	-.04493	-.03209
.39923	.09495	.06782	.40077	-.04497	-.03212
.44962	.09495	.06782	.45038	-.04385	-.03132
.5000	.09290	.06636	.50000	-.04143	-.02959
.55035	.08869	.06335	.54965	-.0376	-.02685
.60064	.08266	.05904	.59936	Linear	Linear
.65086	.07513	.05367	.64914	↓	↓
.70101	.06634	.04738	.69899		
.75107	.05655	.04039	.74893		
.80103	.04591	.03279	.79897		
.85090	.03470	.02478	.84910		
.90066	.02309	.01649	.89934		
.95033	.01150	.00822	.94967		
1.000	0	0	1.00000	0	0

TABLE II.- COORDINATES OF INSIDE SLAT[1] AND WING PARALLEL TO THE MODEL
PLANE OF SYMMETRY

[Outside coordinates are the same as those in table I]

x/c	$\eta = 0$		$\eta = 1.0$	
	Slat z/c	Wing z/c	Slat z/c	Wing z/c
0.02262	-0.01592	-0.01592	-0.01183	-0.01183
.02283	-.01213	-.01460	-.00908	-.01045
.04757	.01873	.01345	.01320	.00935
.07247	.03284	.02945	.02365	.02063
.09746	.04505	.04266	.03190	.02943
.14757	.06526	.06526	.04510	.04318

[1]Slat trailing edge at x/c = 0.1555
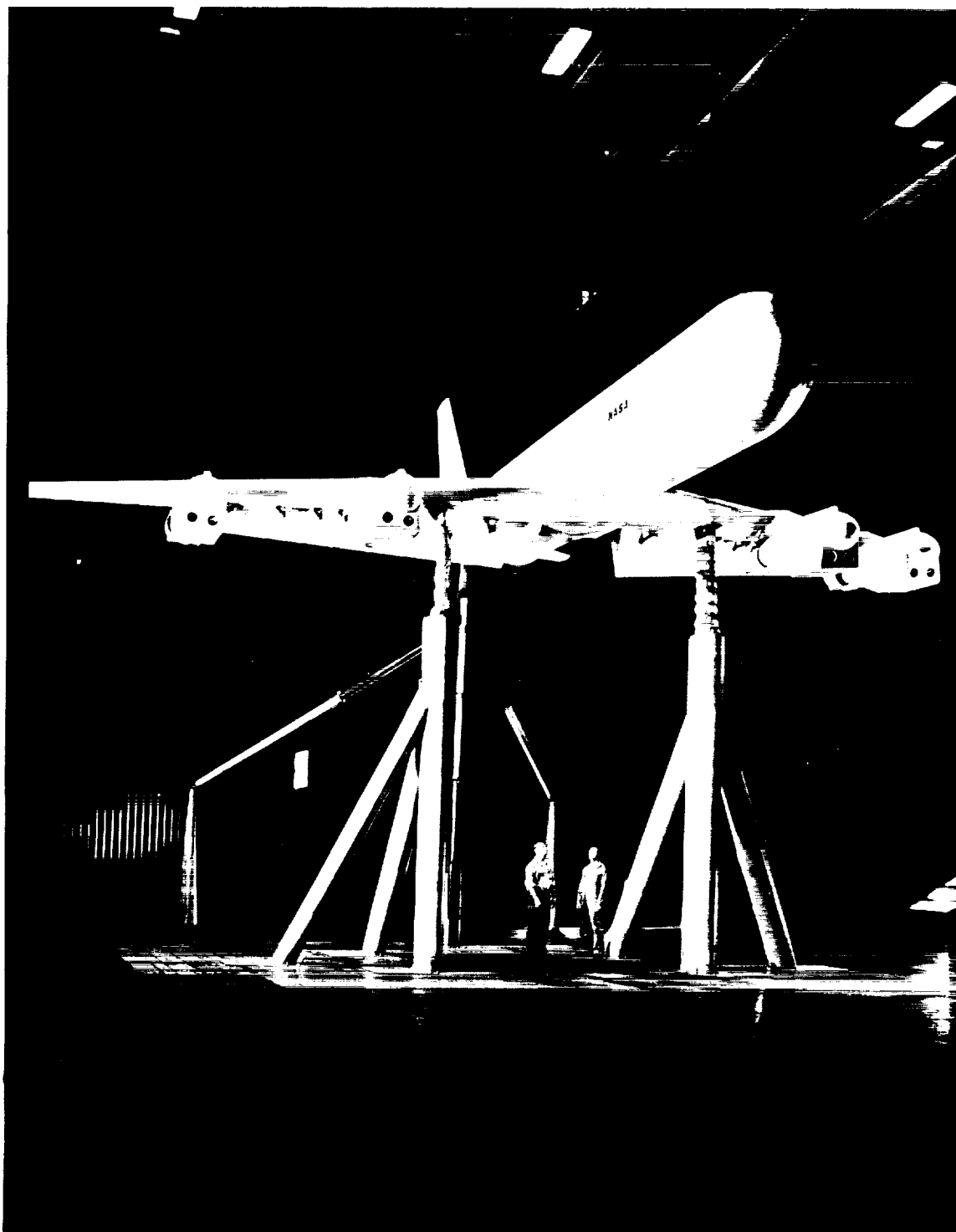
A-24438

Figure 1.- Photograph of the model as mounted in the Ames 40- by 80-Foot
Wind Tunnel.

Moment center

9.20

16.10

35°

35°

7.67

9.45

c/4

21.46

23.00

All dimensions in feet

c/4

c/4

9.86

2.07

.08

2° Wing incidence
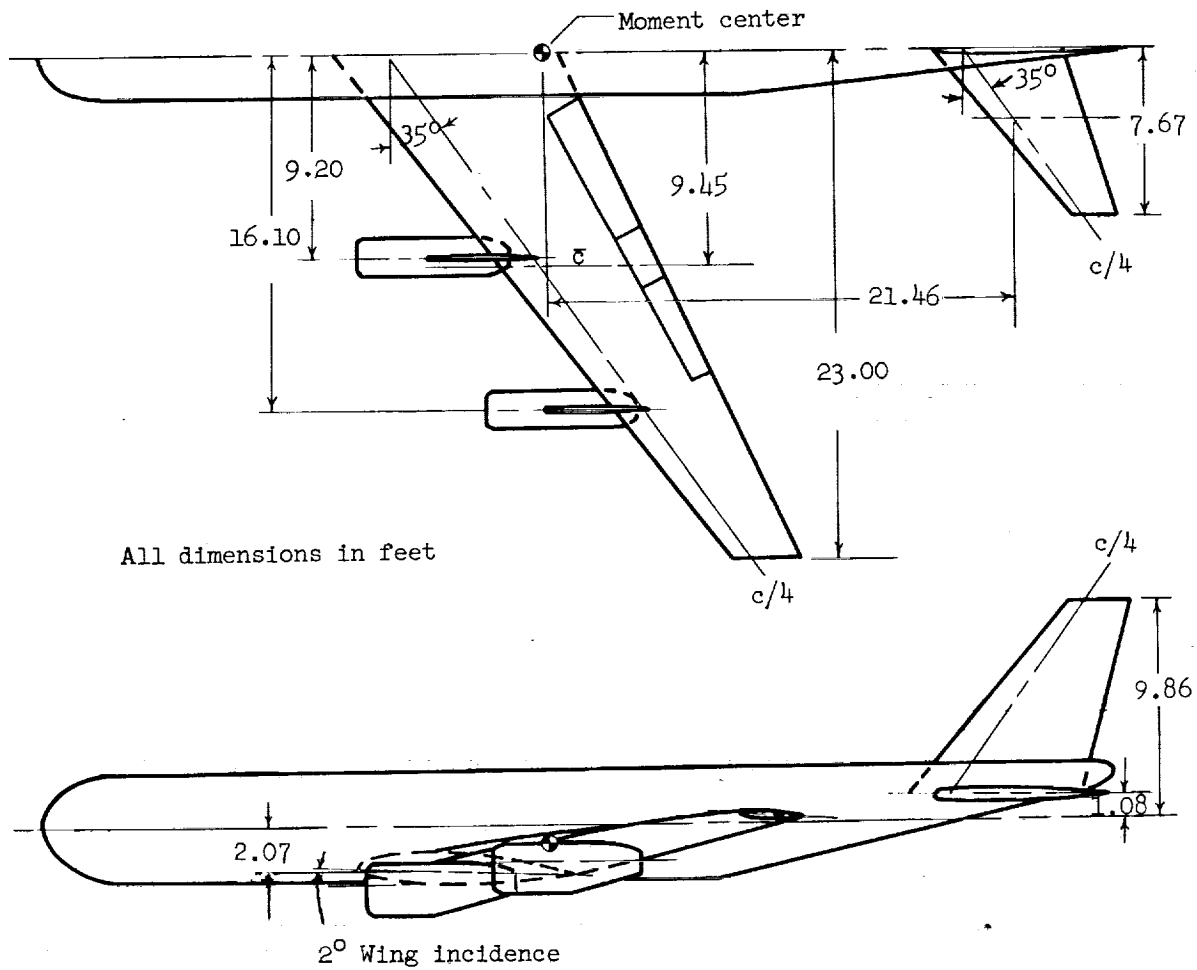
	Wing	Horizontal tail	Vertical tail
Aspect ratio	7.0	3.7	3.3
Taper ratio	0.3	0.375	0.359
Area, sq ft	302.0	62.8	46.7
Mean aerodynamic chord, ft	7.20	4.39	5.72
Dihedral, deg	6.0	0.0	---

Figure 2.- Geometric details of the model.
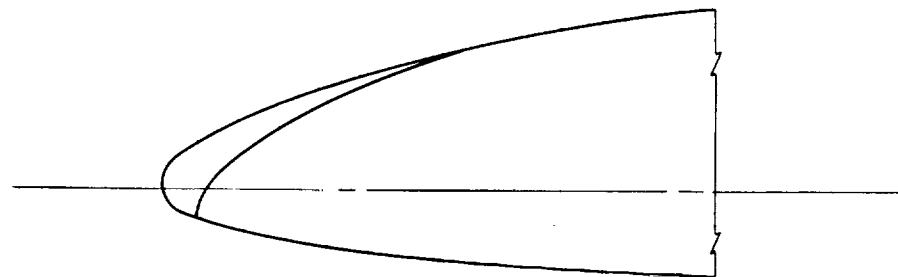
Airfoil section (streamwise)
Root   NACA 65A414
Tip   NACA 65A410

.02c

.14c

$\delta_s=15°$

.0185c

Leading-edge slat deflected
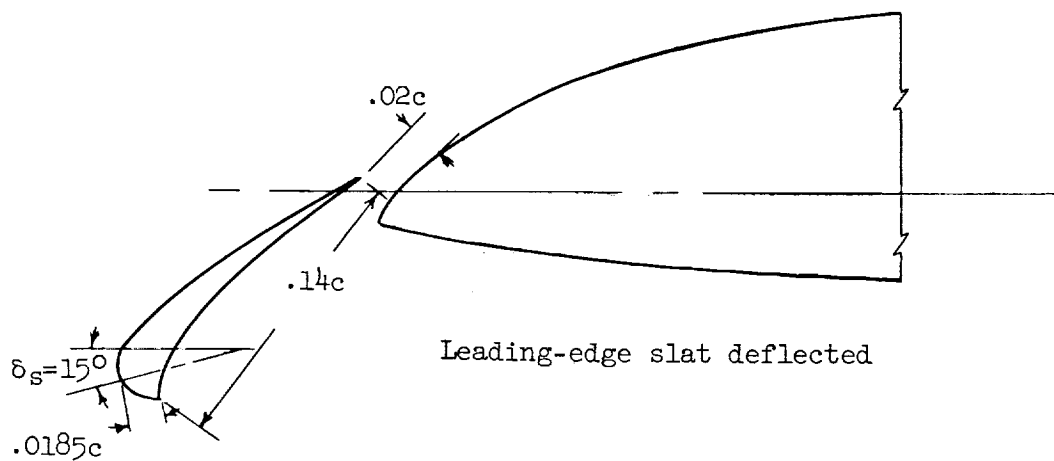
(a) Leading-edge slats.

Figure 3.- Details of the high-lift devices.

Fuselage outline

10.10

23.00

29.61°

Flap hinge line

.4η

.7η

C_L of Model

.09η

.34η

.44η

.63η

All dimensions in feet except as noted

3.03

1.0η

.60c

.68c

δ_f

35°

Nozzle height, .020 inch

90°

Flap chord line

Pivot point of flap

.32c

Section A-A
(Typical)
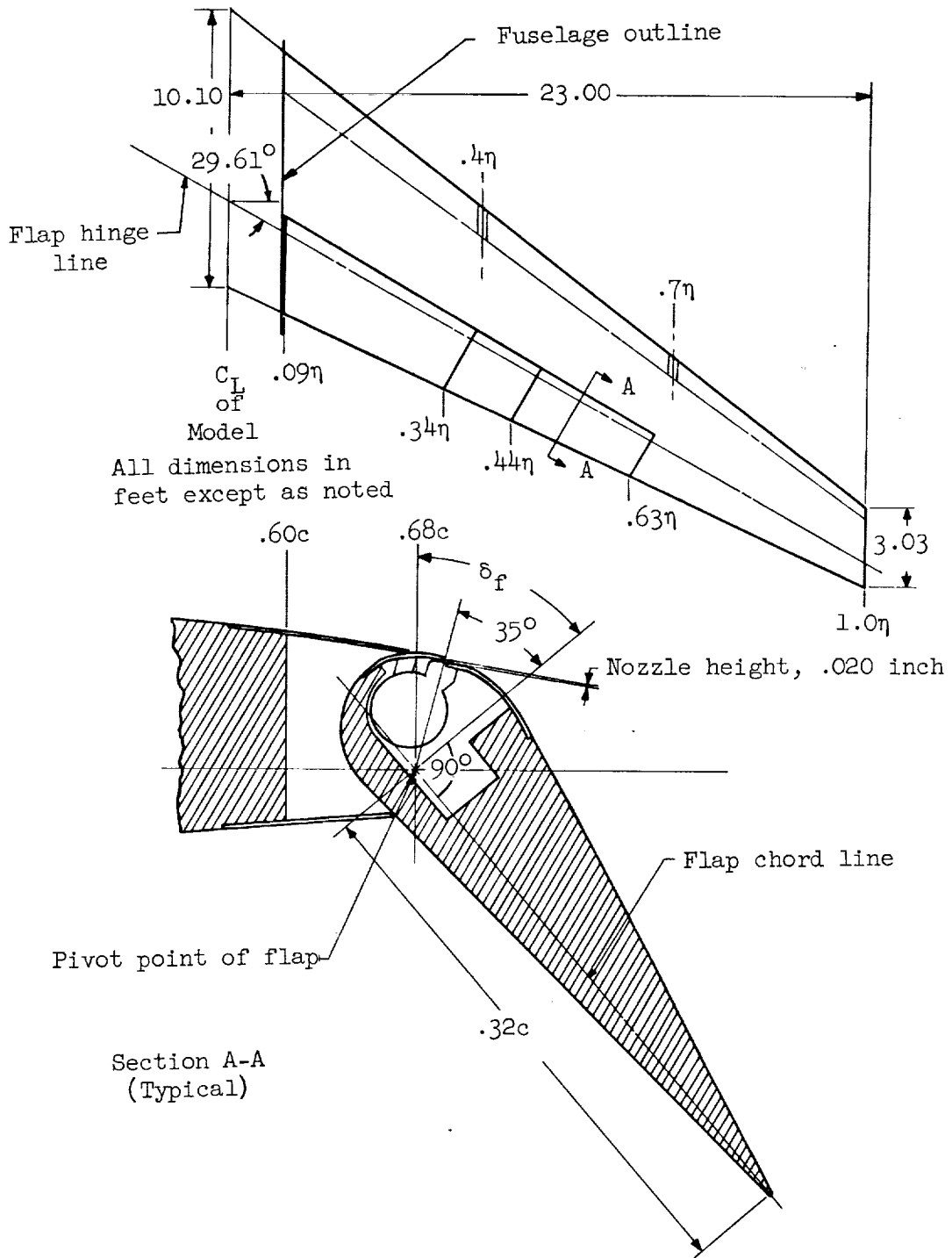
(b) Wing and trailing-edge flap.

Figure 3.- Concluded.
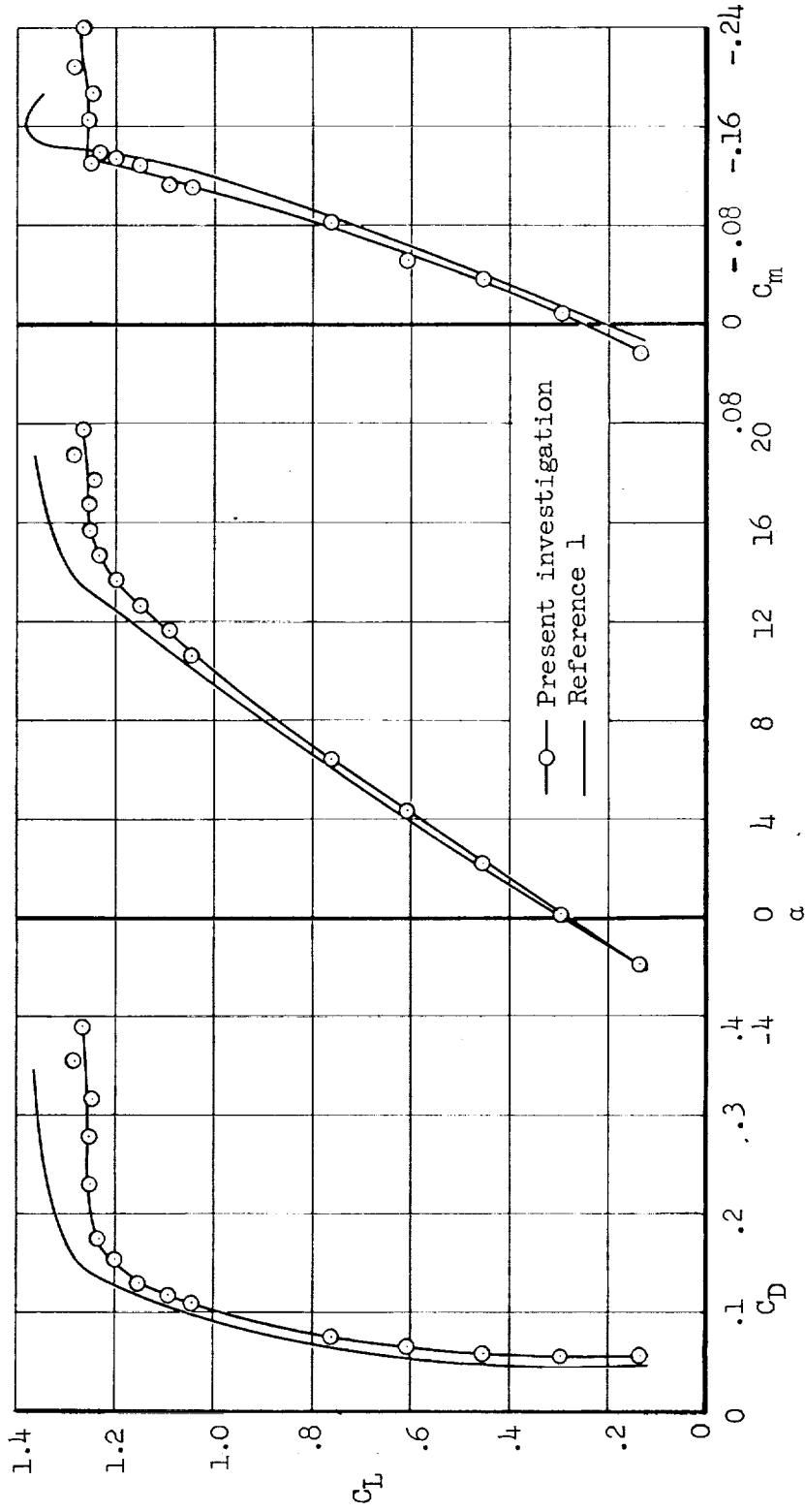
Figure 4.– Longitudinal characteristics of the model; $\delta_f = 0^\circ$, leading-edge slats retracted.
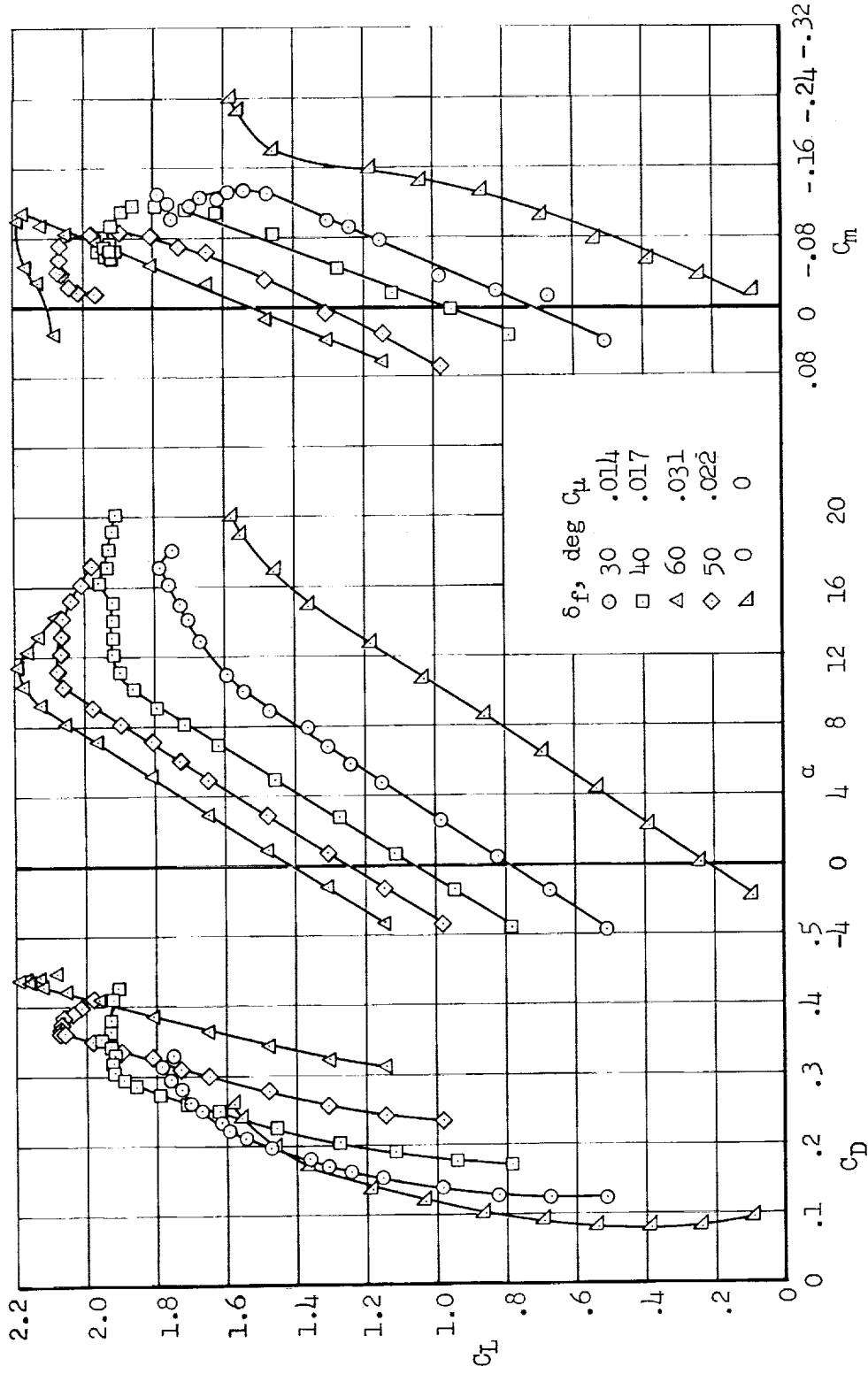
(a) Interrupted-span flap.

Figure 5.- Longitudinal characteristics of the model with several flap deflections, boundary-layer control, and leading-edge slats.

A
3
4
0
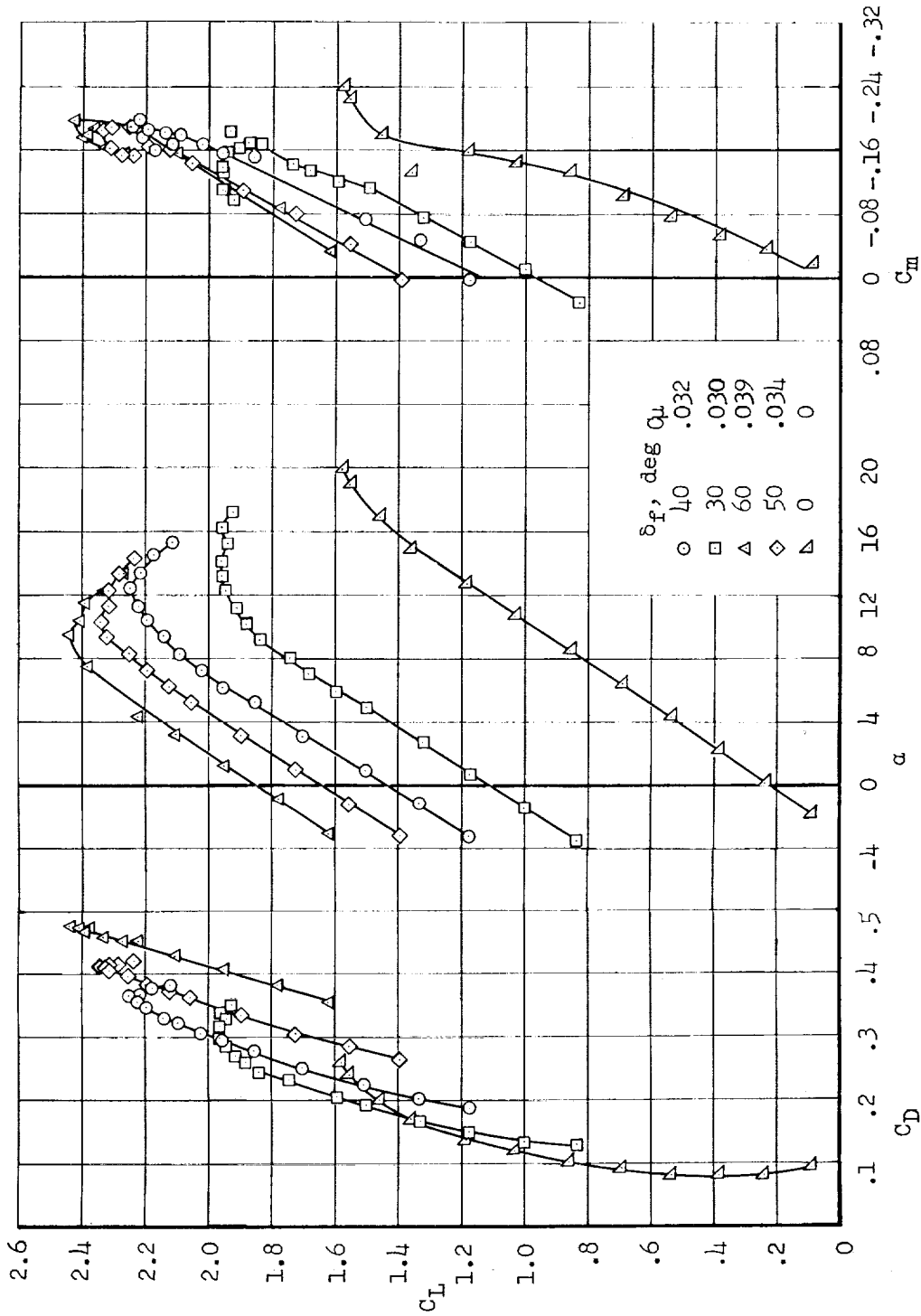
(b) Continuous-span flap.

Figure 5.- Concluded.
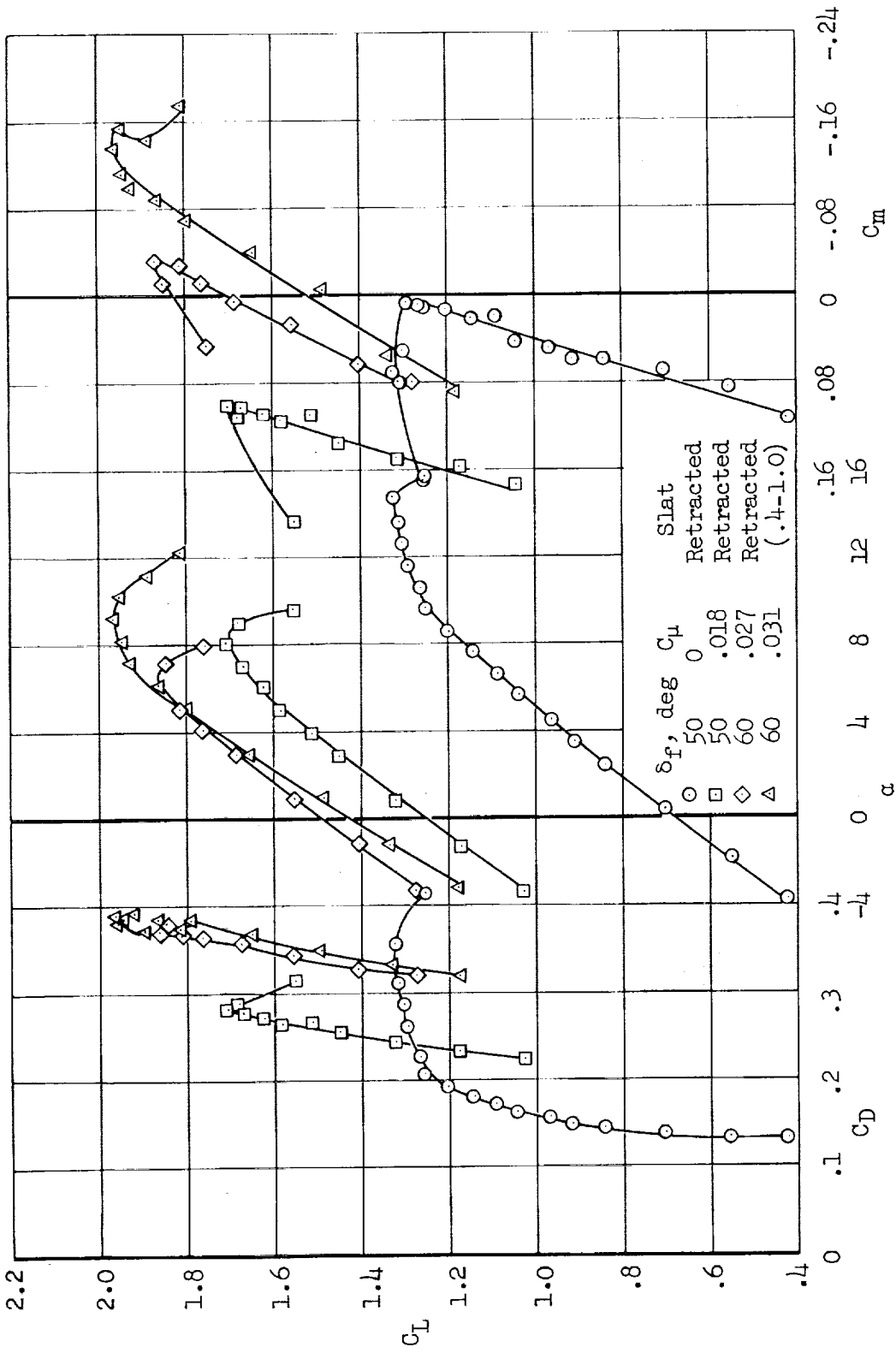
Figure 6.- Effect of boundary-layer control and partial-span slats on the longitudinal character-istics of the model with the interrupted-span flap.

A
3
4
0
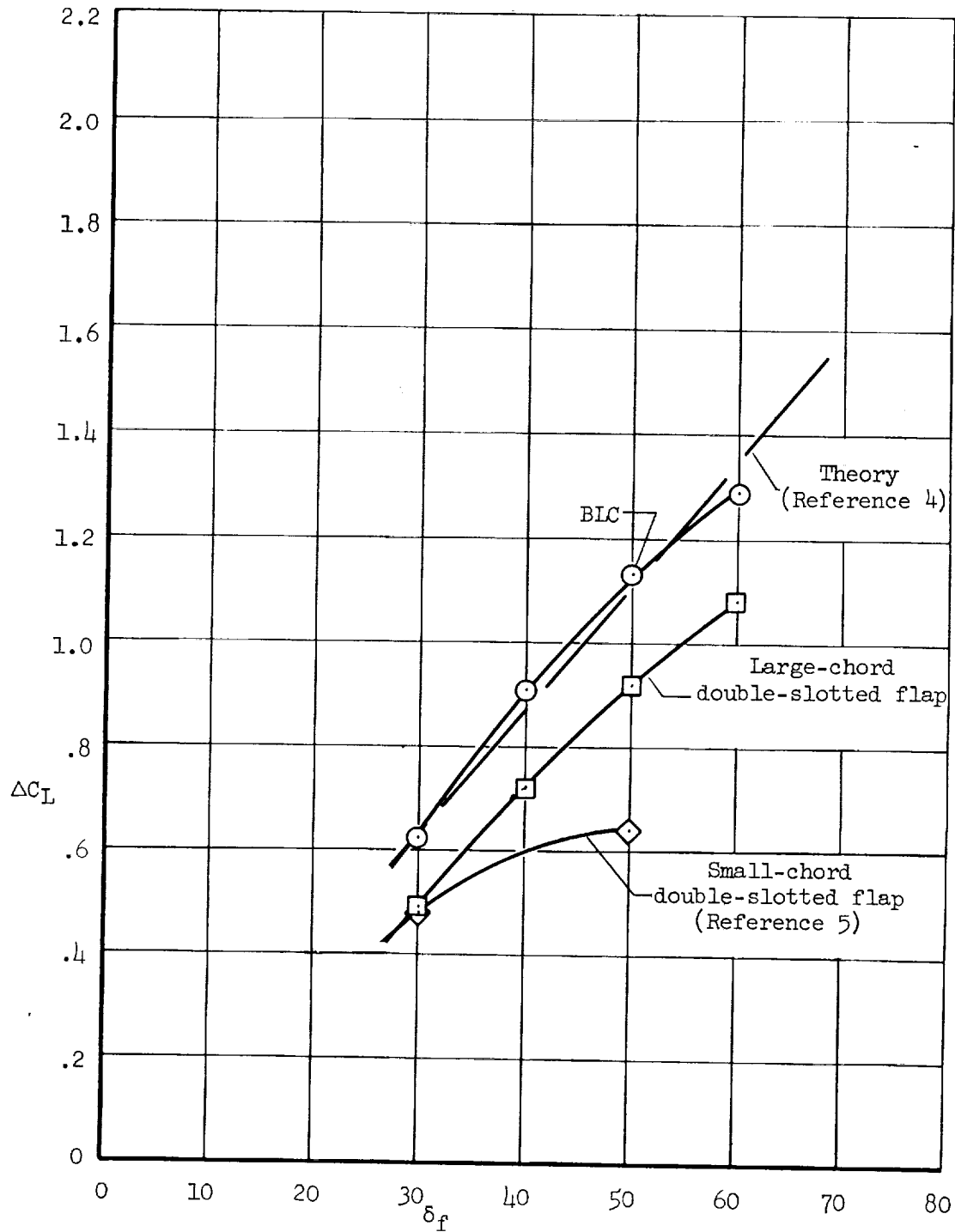
(a) Interrupted-span flap.

Figure 7.- Variation of flap lift increment with flap deflection; $\alpha = 0^\circ$, horizontal tail off.
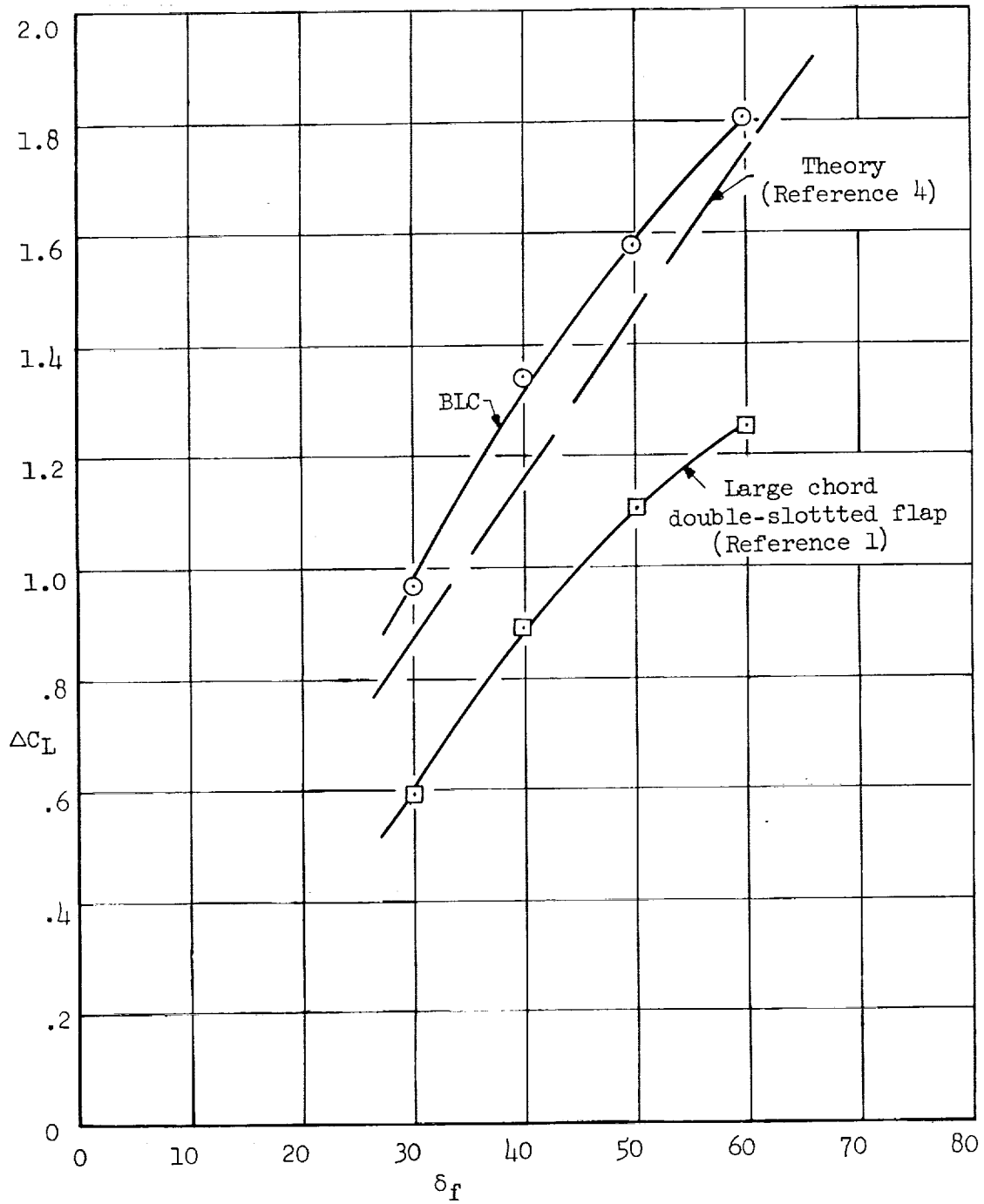
(b) Continuous-span flap.

Figure 7.- Concluded.
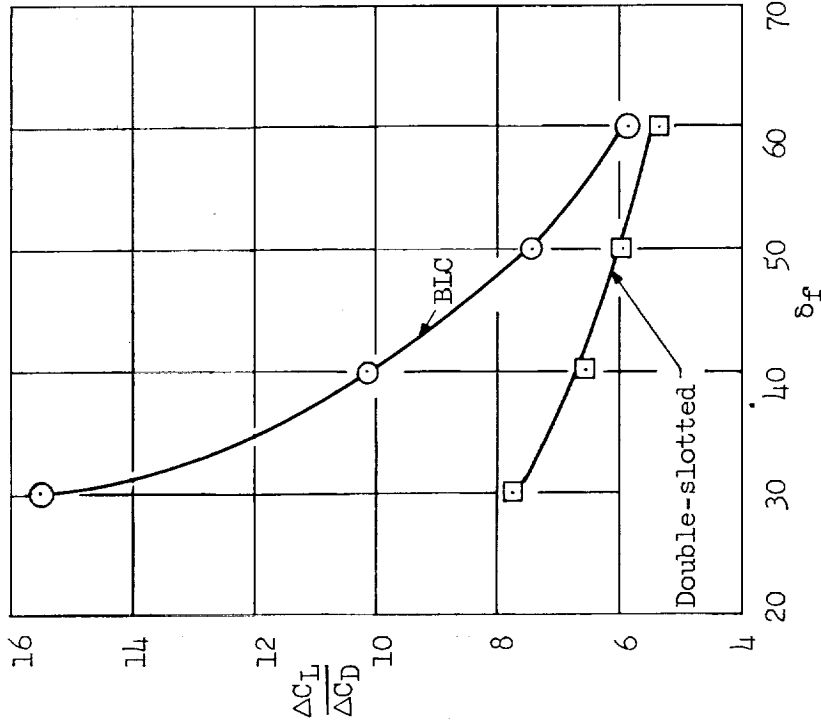
(a) Interrupted-span flap.
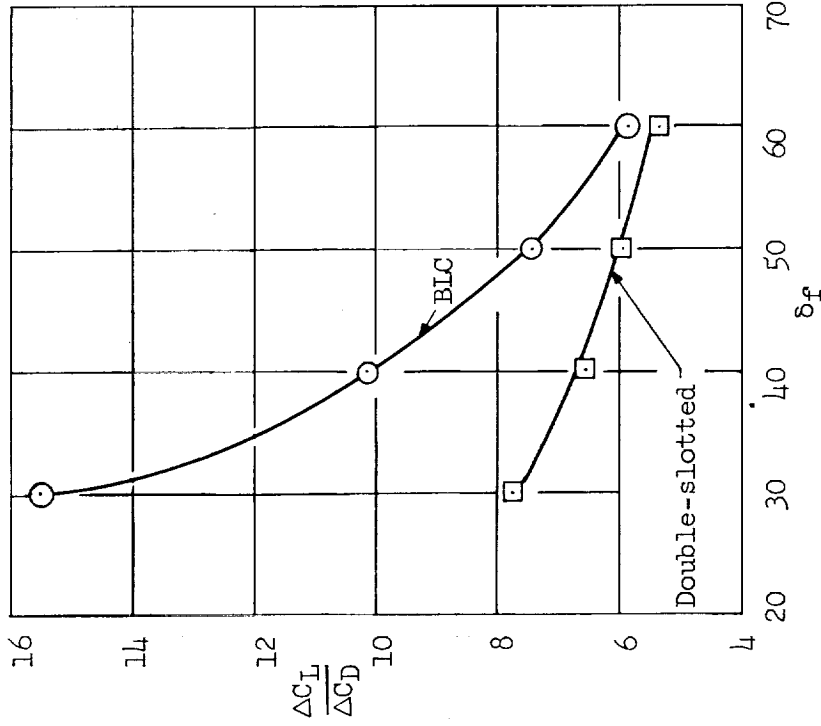
(b) Continuous-span flap.

Figure 8.- Variation of flap incremental lift to drag ratio with deflection; $\alpha = 0^\circ$, horizontal tail off.
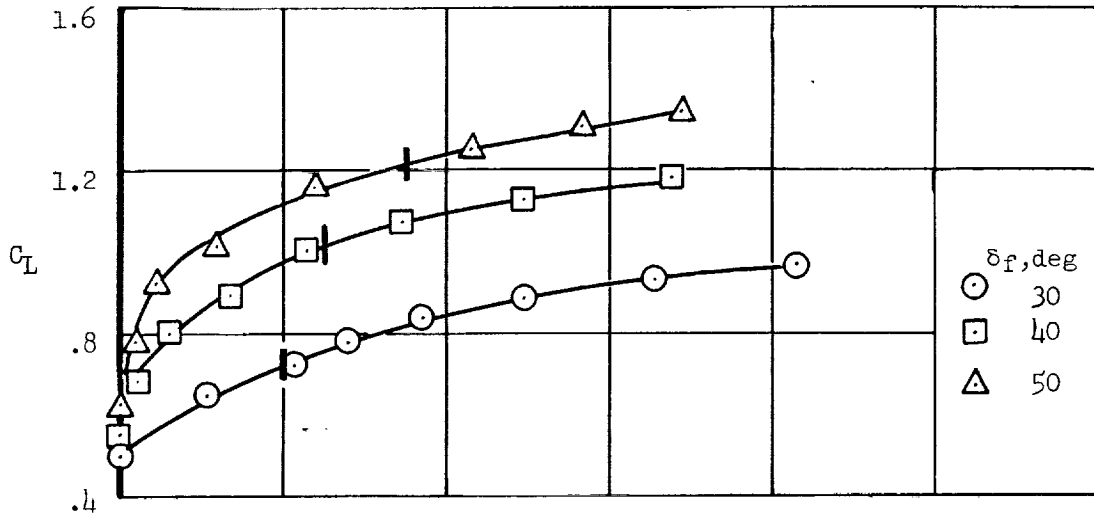
(a) Interrupted-span flap.
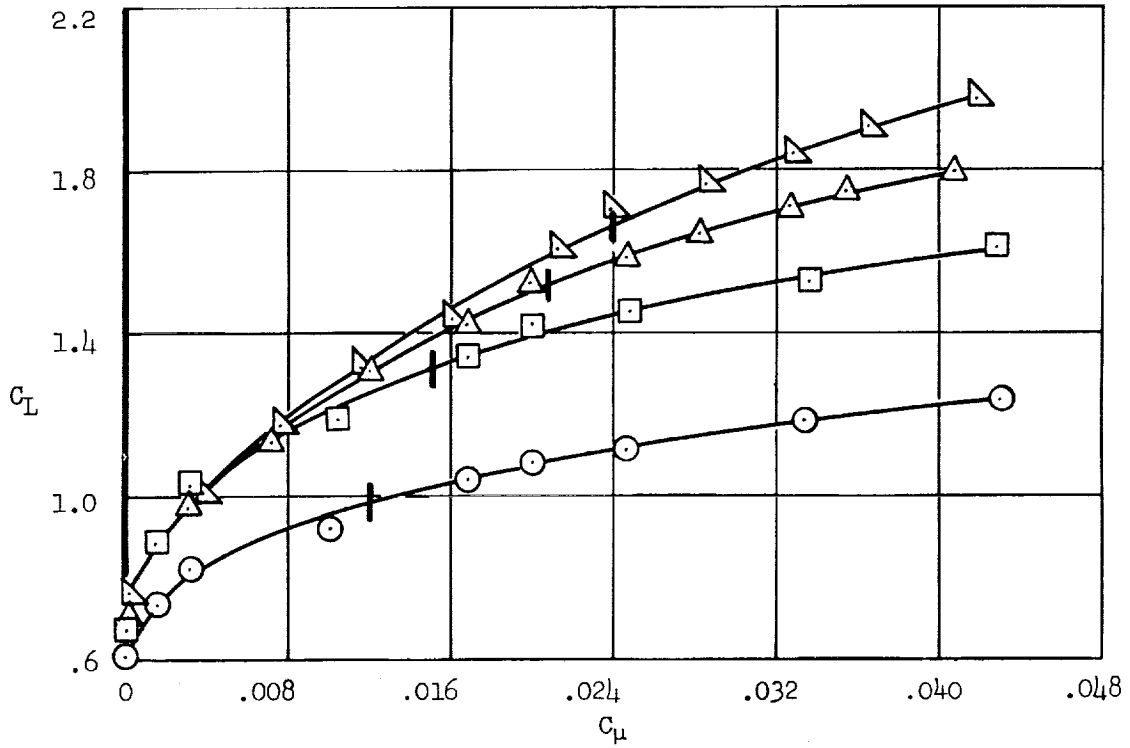
Figure 9.- The variation of lift coefficient with momentum coefficient; $\alpha = 0^\circ$, slats extended.
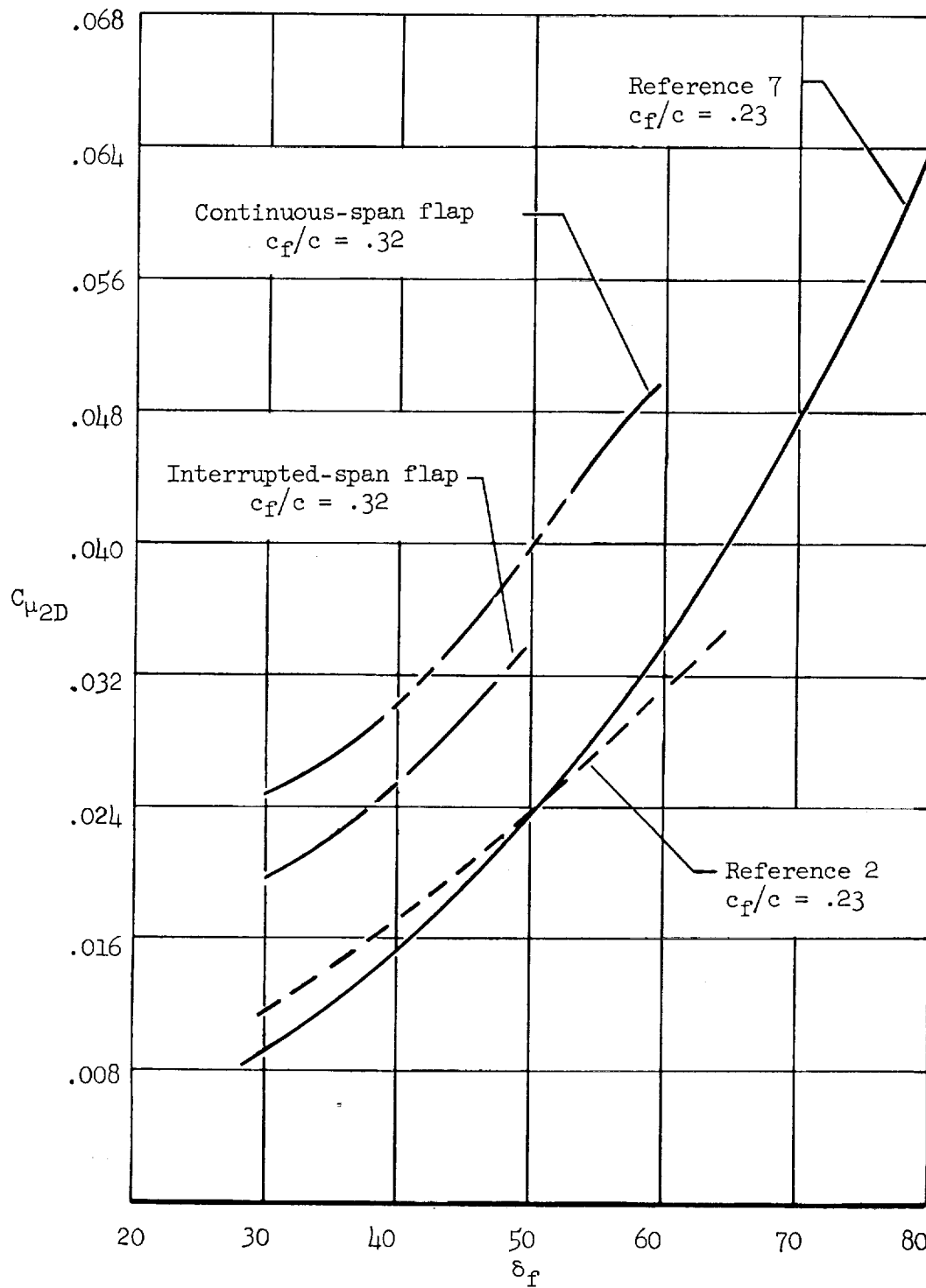
Figure 10.- Variation of two-dimensional momentum coefficient with flap deflection.
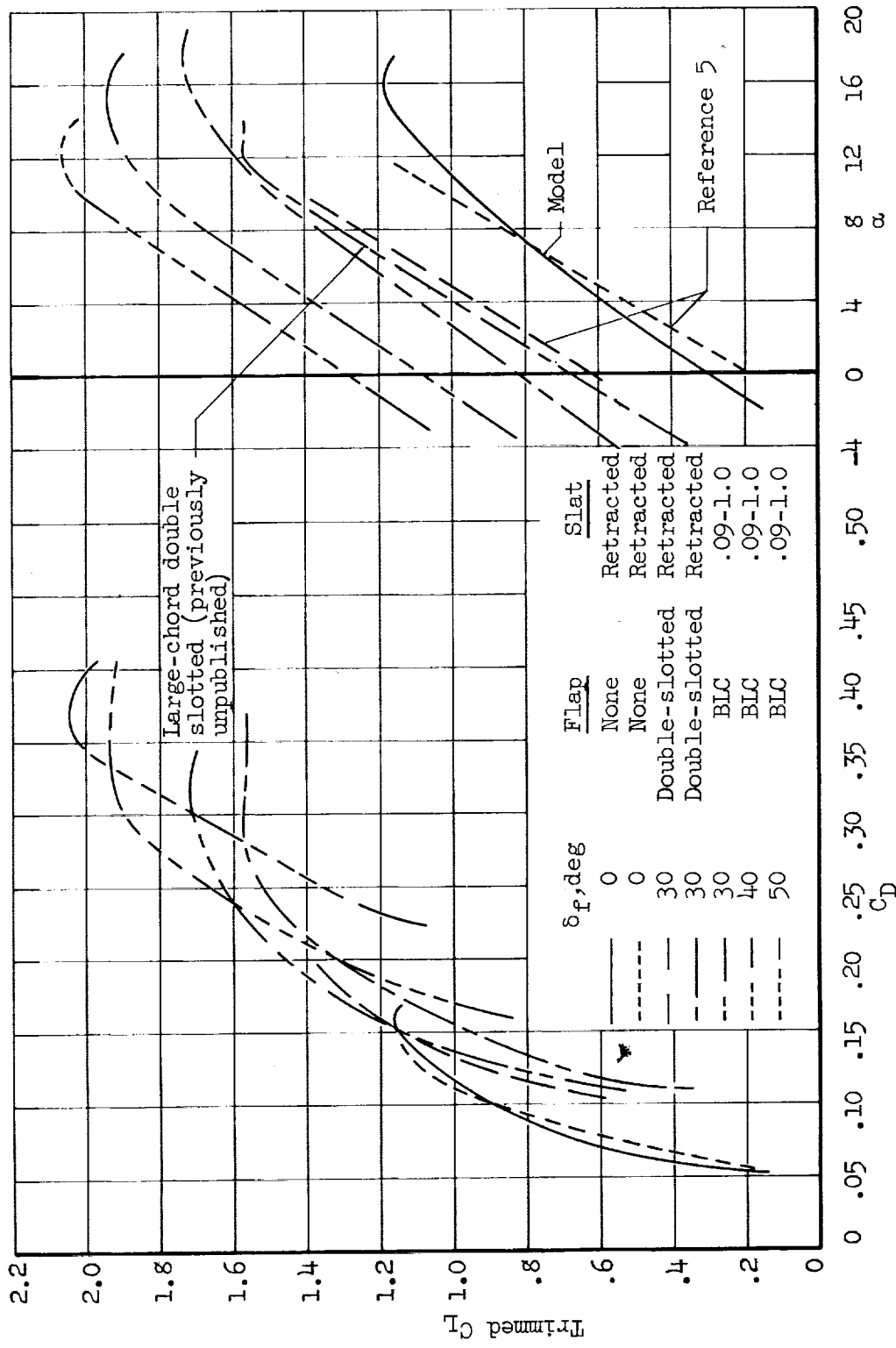
Figure 11.- Longitudinal characteristics used for performance computation; interrupted-span flap.
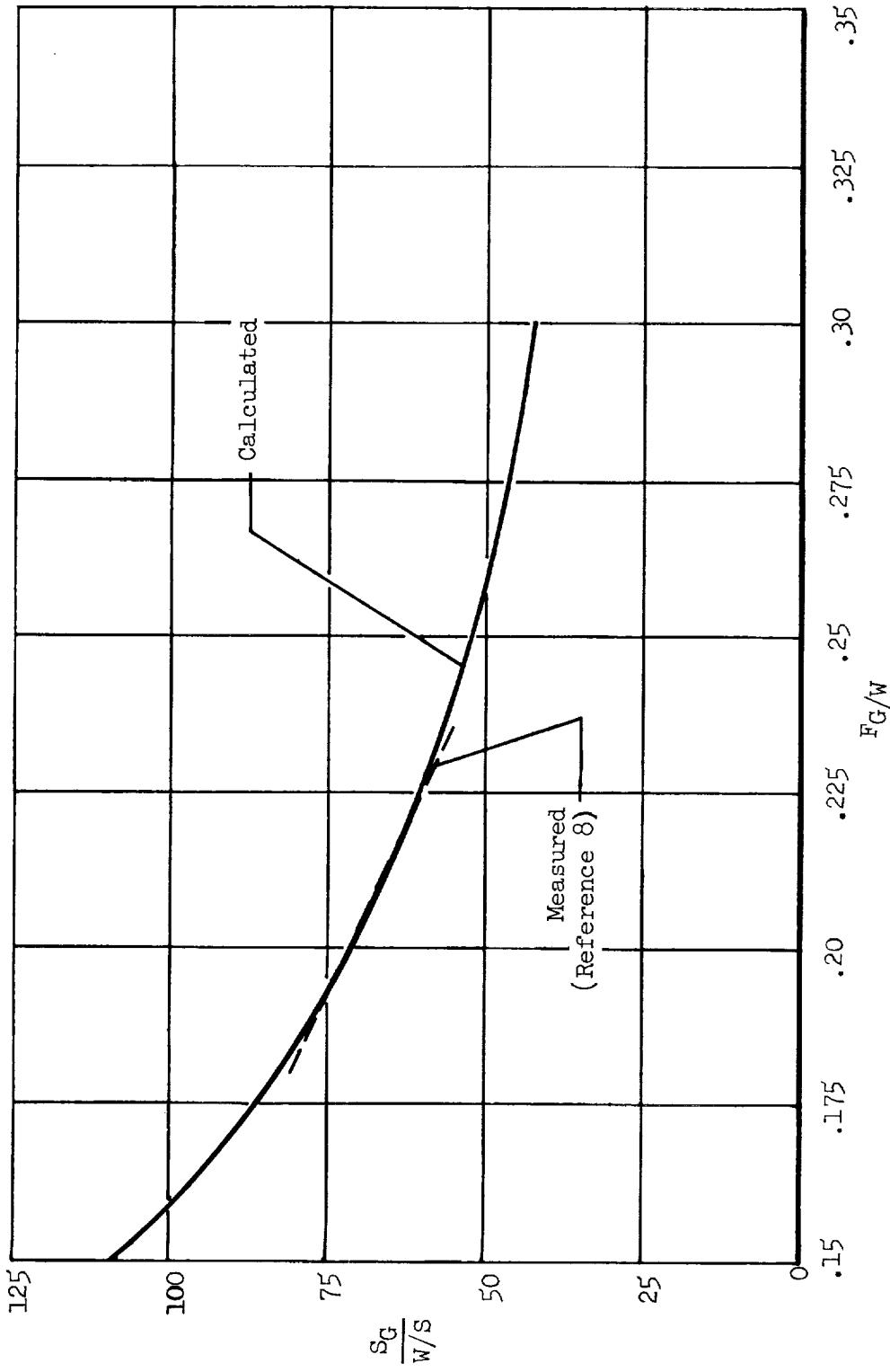
Figure 12.- Comparison of measured and calculated take-off ground-roll distance for a range of thrust to weight ratios; $\delta_f = 30°$.

(a) Two-position ducting valve.
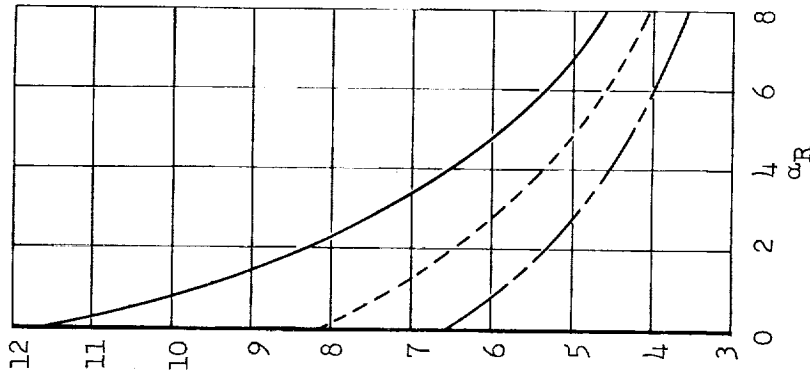
(b) Programmed bleed.
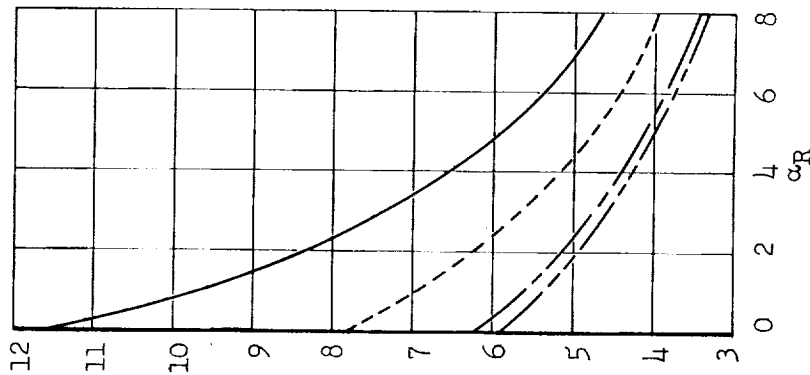
(c) Auxiliary compressor.

Figure 13.- Effect of angle of rotation on take-off ground-roll distance for various flap configurations; $W/S = 100$ lb/sq ft, $F_G/W = 0.206$.

Figure 14.- Effect of angle of rotation on take-off ground-roll distance for various flap configurations; W/S = 100 lb/sq ft, F_G/W = 0.25.

(a) $F_G/W = 0.206$.

Legend:
- ⊙ Double-slotted flap
- ⊡ BLC flap - two-position bleed valve
- ◇ BLC flap - programmed bleed
- △ BLC flap - auxiliary compressor
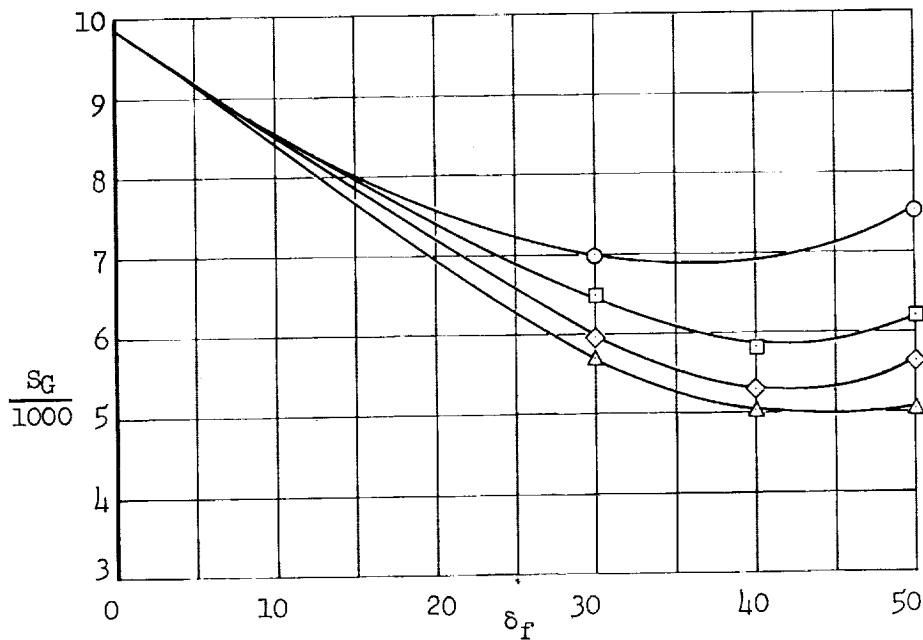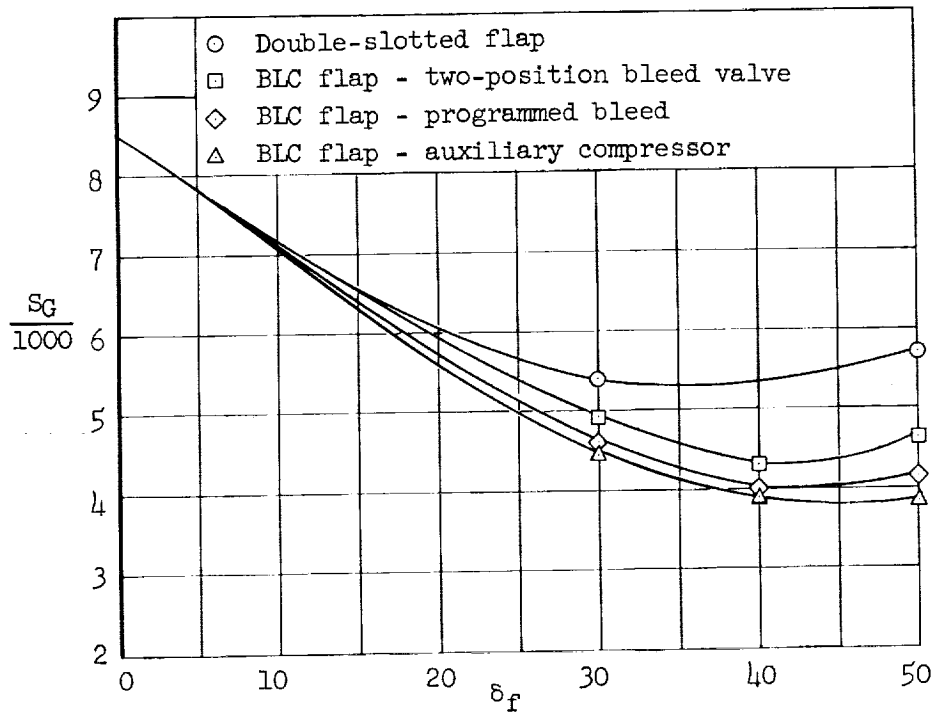
(b) $F_G/W = 0.25$.

Figure 15.- Variation of take-off ground-roll distance with flap deflection for several flap configurations; $\alpha_R = 6°$, $W/S = 100$ lb/sq ft.

A
3
4
0

Tick marks indicate 35 foot altitude

(a) Four engine.

$\delta_f=40°$ BLC and slats extended
$\delta_f=30°$ BLC and slats extended
$\delta_f=30°$ Double-slotted flaps
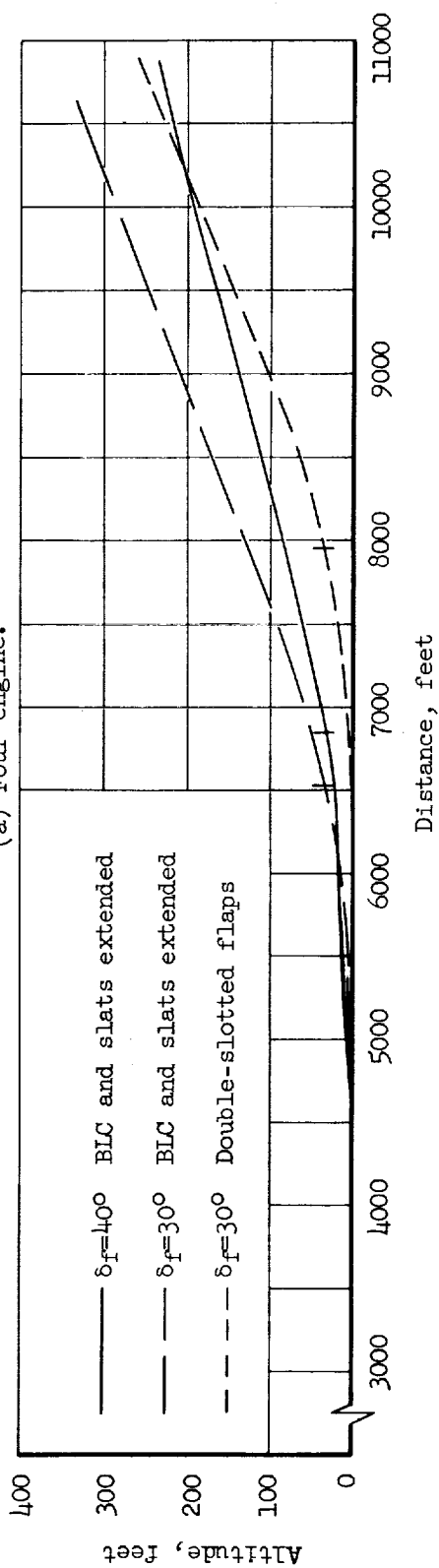
(b) One engine inoperative.

Figure 16.- Effect of high-lift devices on take-off and climbout with programmed engine bleed air used for boundary-layer control; $F_G/W = 0.25$, $W/S = 100$ lb/sq ft.

(a) Four engine.

(b) One engine inoperative.

Tick marks indicate 35 foot altitude

————— $\delta_f = 40^\circ$ BLC and slats extended

————— $\delta_f = 30^\circ$ BLC and slats extended

— — — $\delta_f = 30^\circ$ Double-slotted flaps

Figure 17.- Effect of high-lift devices on take-off and climbout with an auxiliary compressor for boundary-layer control; $F_G/W = 0.25$, $W/S = 100$ lb/sq ft.

A
3
4
0

Tick marks indicate 35 foot altitude

Altitude, feet

400

300

200

100

0

5000   6000   7000   8000   9000   10000   11000   12000   13000

Distance, feet

(a) Four engine.

$\delta_f = 40°$ BLC and slats extended

$\delta_f = 30°$ BLC and slats extended

$\delta_f = 30°$ Double-slotted flaps

Altitude, feet

400

300

200

100

0

5000   6000   7000   8000   9000   10000   11000   12000   13000

Distance, feet

(b) One engine inoperative.

Figure 18.— Effect of high-lift devices on take-off and climbout with programmed engine bleed air used for boundary-layer control; $F_G/W = 0.206$, $W/S = 100$ lb/sq ft.
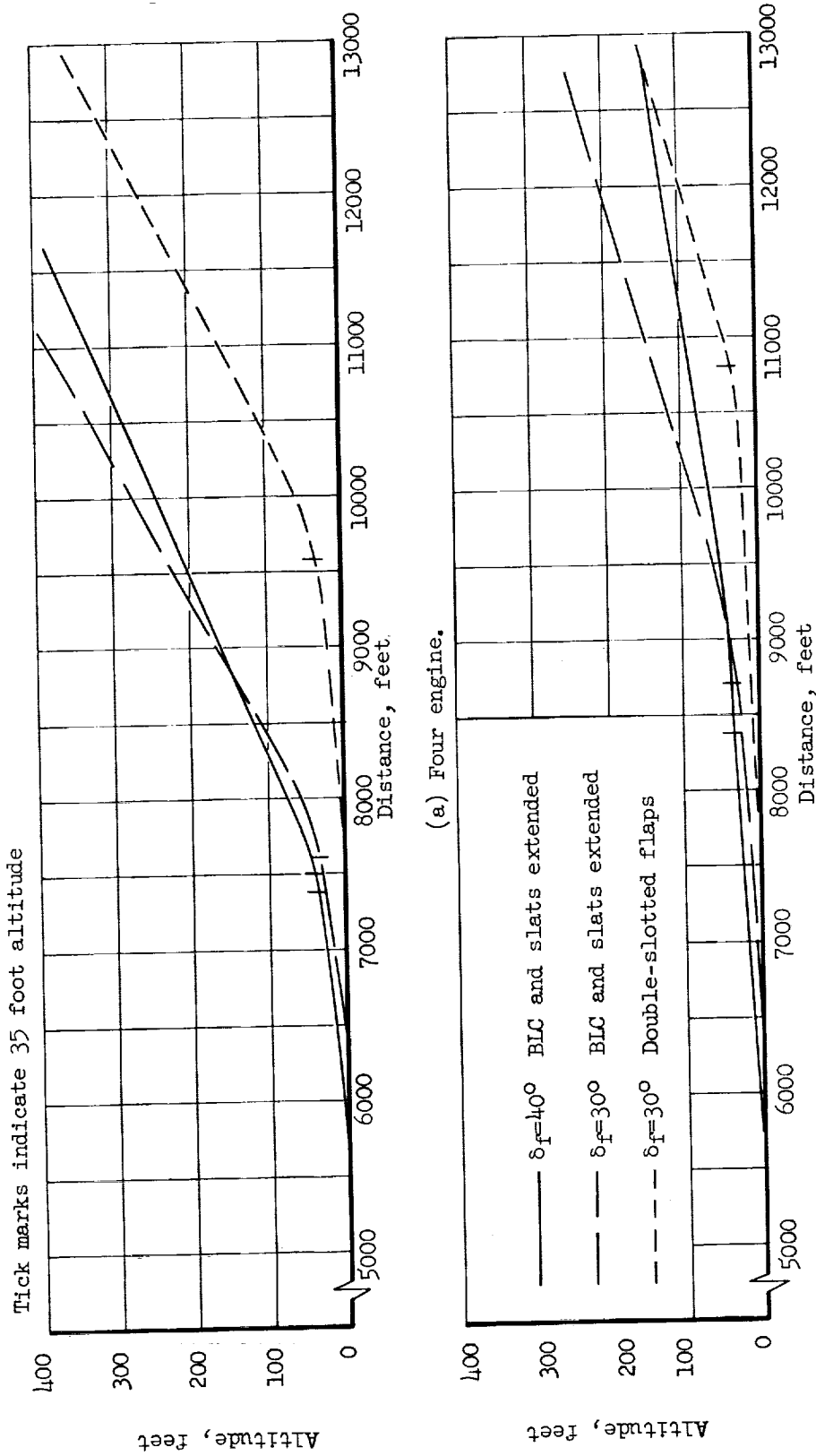
Figure 19.- Effect of high-lift devices on take-off and climbout with an auxiliary compressor used for boundary-layer control; F_G/W = 0.206, W/S = 100 lb/sq ft.
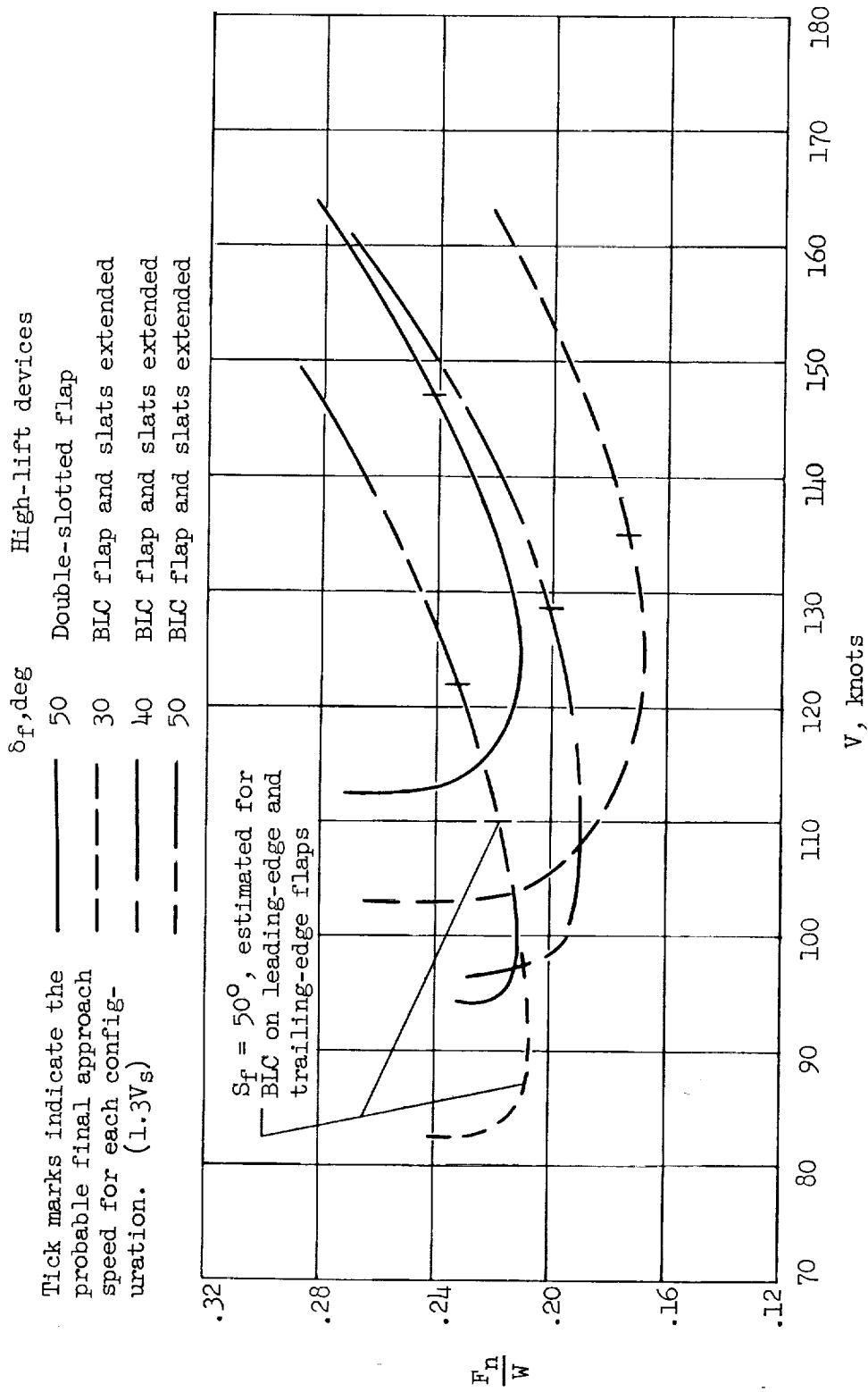
Figure 20.- The thrust to weight ratio required for level flight for several flap configurations; W/S = 65 lb/sq ft.
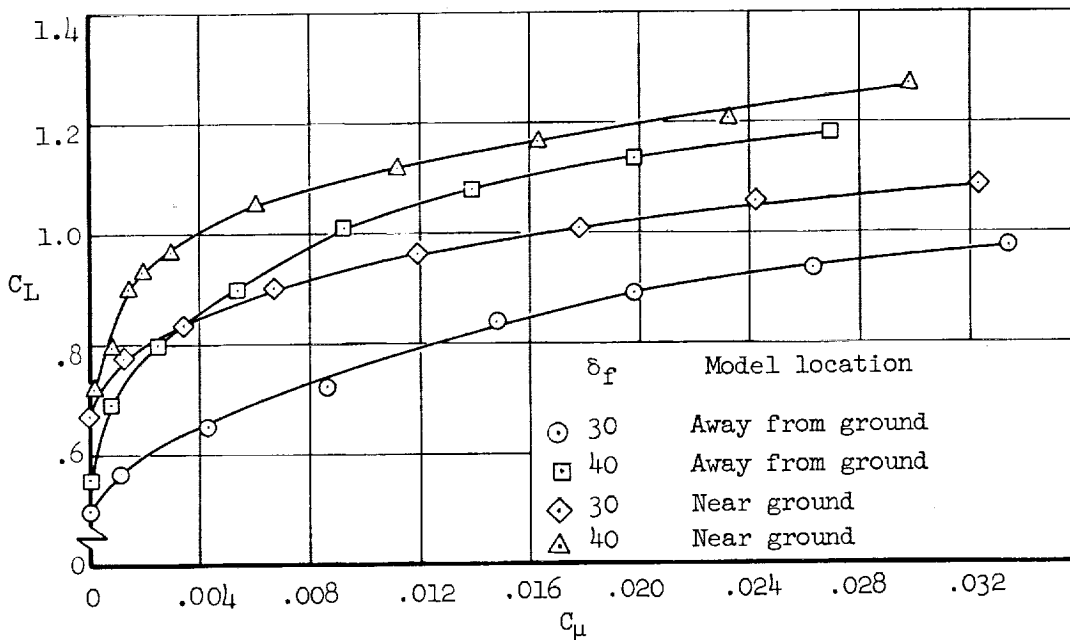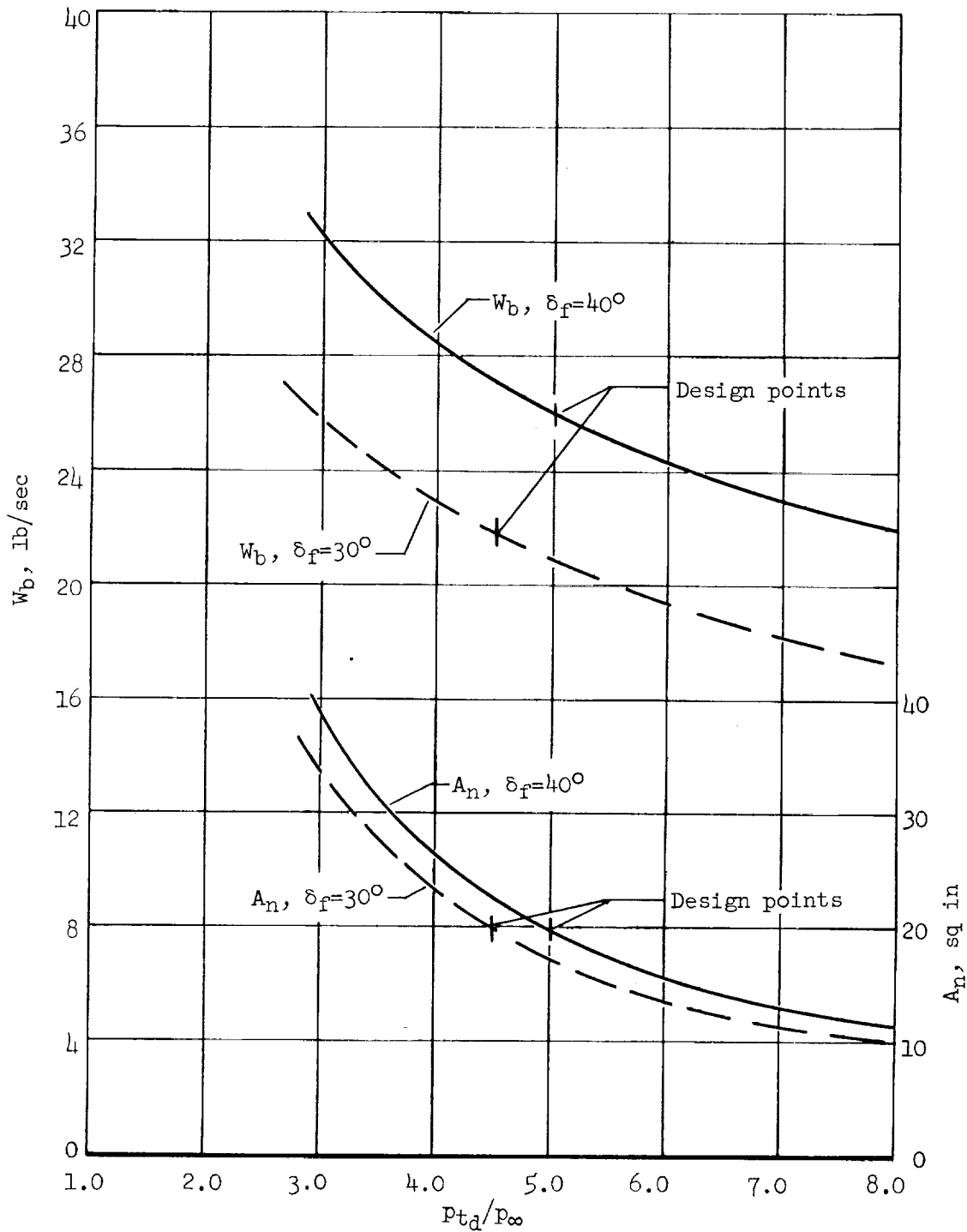
(a) Variation of C_L with C_μ.
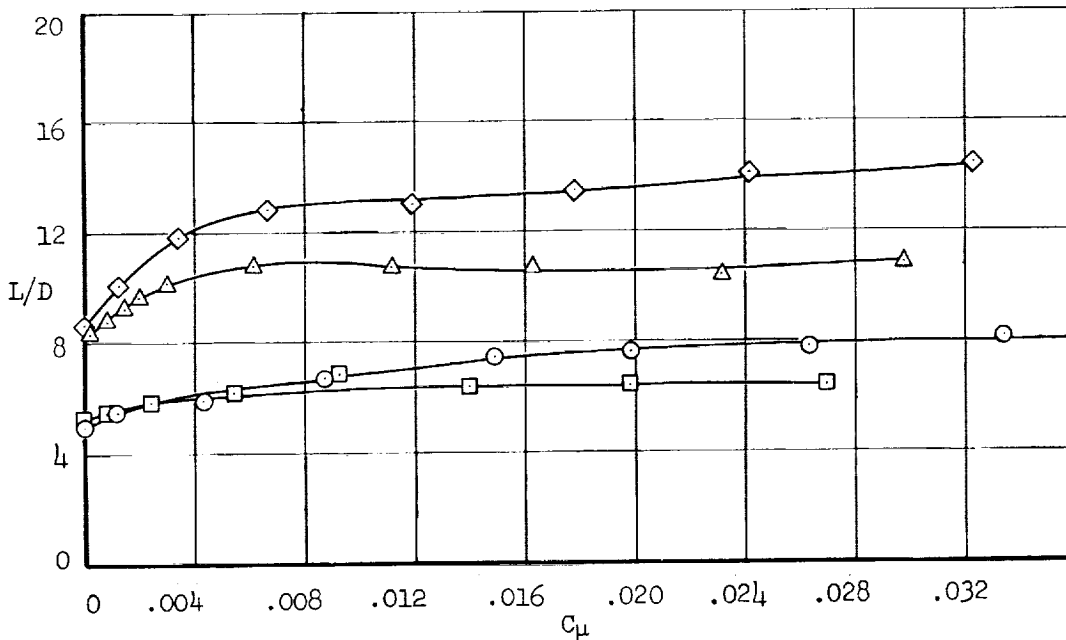
(b) Variation of L/D with C_μ.
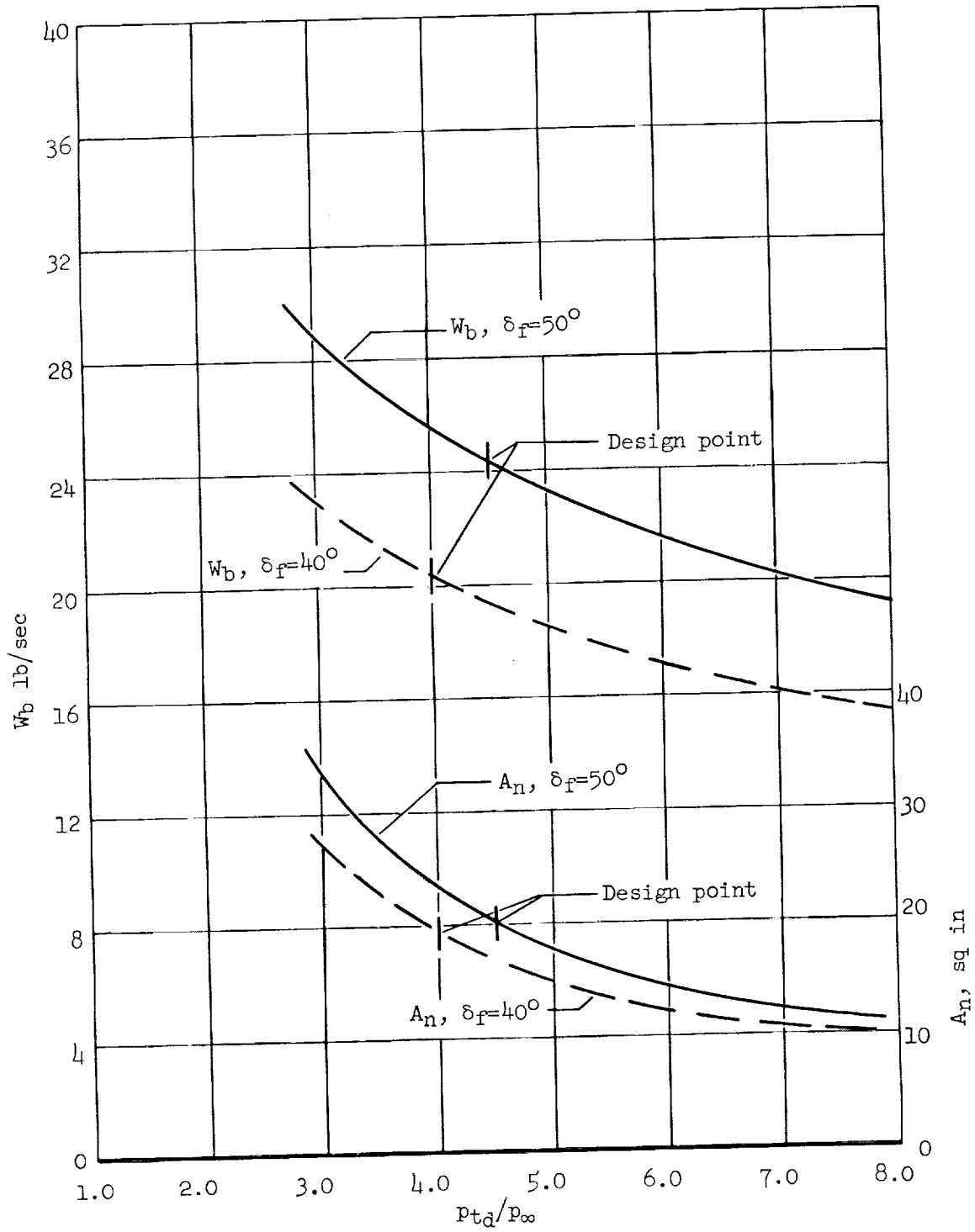
Figure 21.- Effect of ground on the variation of lift coefficient and lift-drag ratio with momentum coefficient; $\alpha = 0^\circ$.
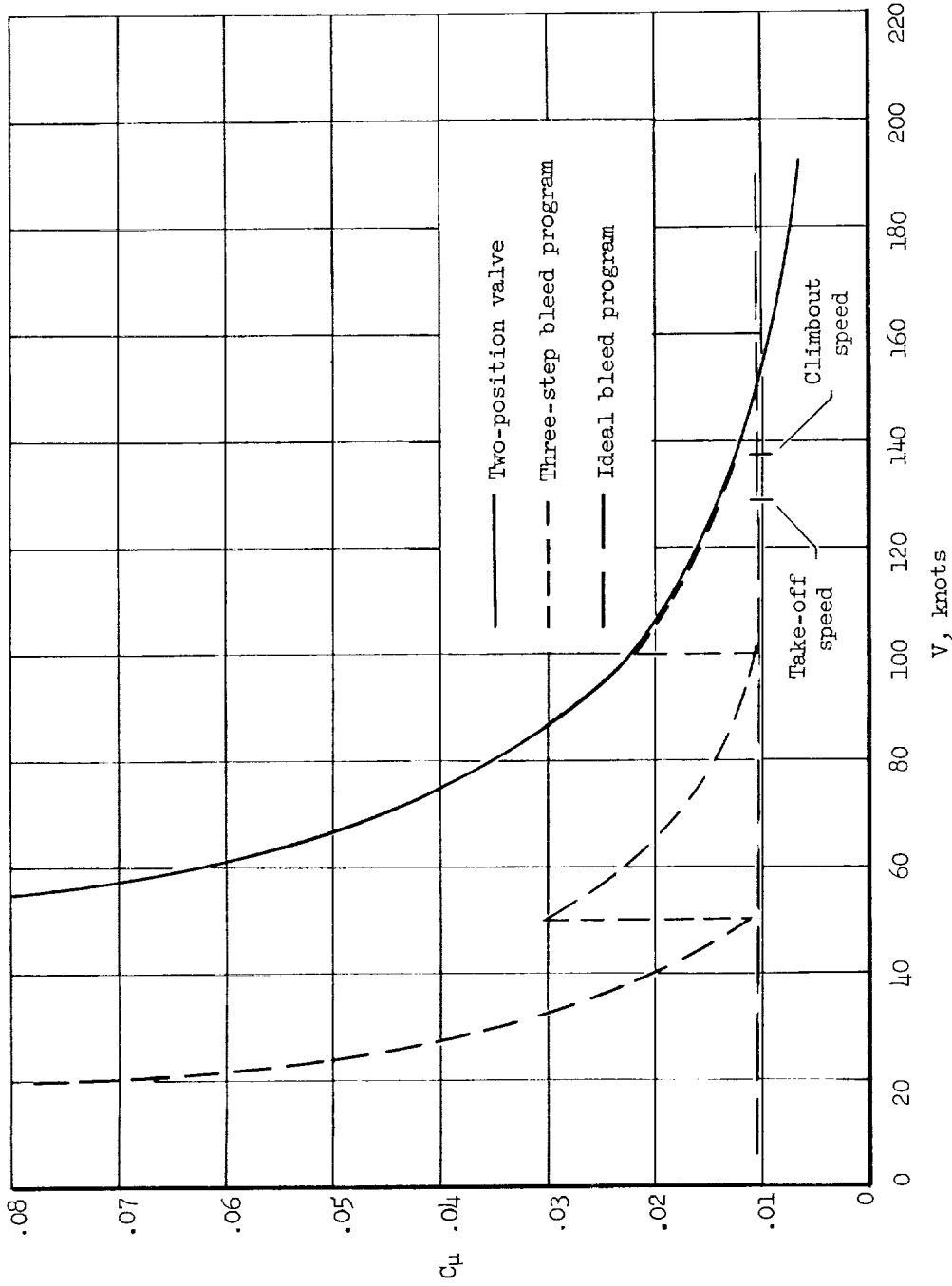
(a) Take-off, W/S = 100 lb/sq ft.

Figure 22.- Variation of bleed air flow rate and nozzle area with blowing pressure.

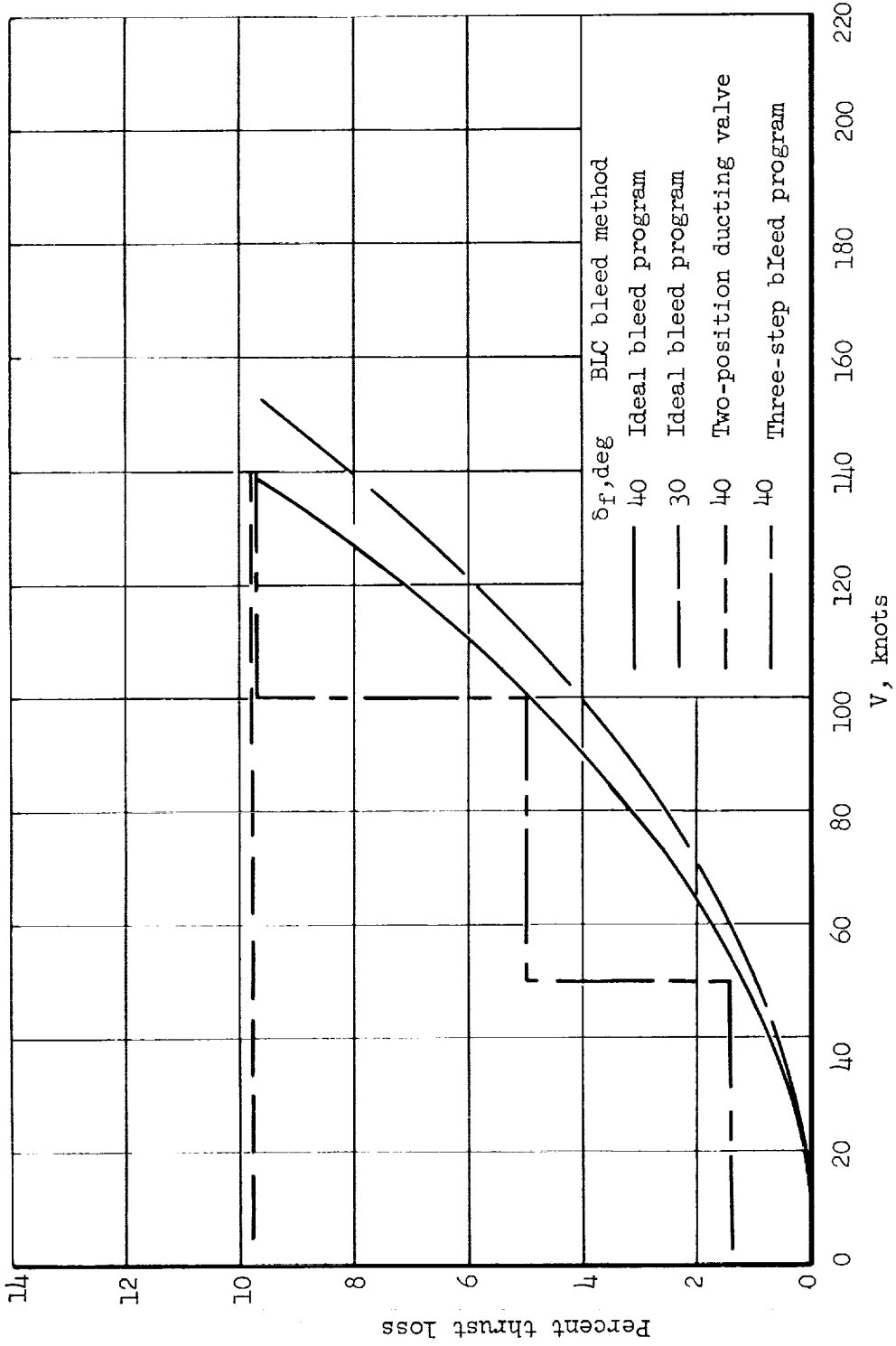(b) Landing, W/S = 65 lb/sq ft.

Figure 22.- Concluded.

A
3
4
0

(a) Variation of C_μ, $\delta_f = 40°$.

Figure 23.- The variation of C_μ and thrust loss with take-off ground-roll velocity for three methods of controlling bleeding air from the engine for boundary-layer control.

(b) Thrust loss.

Figure 23.- Concluded.